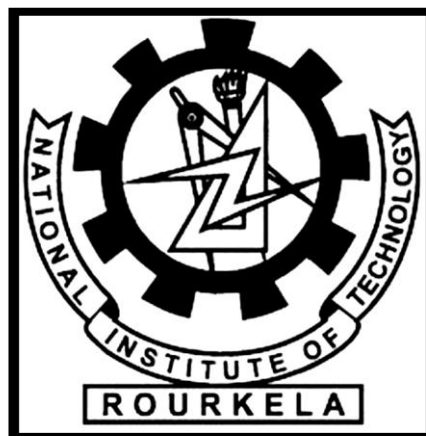


QUANTIFICATION OF CRACKS AND SHRINKAGE USING IMAGE ANALYSIS

*A Thesis Submitted in Partial Fulfilment of the Requirements
for the Degree of*

**Master of Technology
In
Civil Engineering**



Abhishek Tiwari

**DEPARTMENT OF CIVIL ENGINEERING
NATIONAL INSTITUTE OF TECHNOLOGY, ROURKELA
MAY-2015**

QUANTIFICATION OF CRACKS AND SHRINKAGE USING IMAGE ANALYSIS

*A thesis
Submitted by*

**Abhishek Tiwari
(213CE1054)**

*In partial fulfilment of the requirements
for the award of the degree of*

Master of Technology

In

Civil Engineering

(Geotechnical Engineering)

Under the Guidance of

Prof. S.P. Singh



**Department of Civil Engineering
National Institute of Technology, Rourkela**

Odisha -769008, India

May 2015



**NATIONAL INSTITUTE OF TECHNOLOGY ROURKELA,
ODISHA -769008, INDIA**

This is to certify that the thesis entitled, “Quantification of Cracks and Shrinkage using Image Analysis” submitted by Abhishek Tiwari in partial fulfilment of the requirement for the award of Master of Technology degree in Civil Engineering with specialization in Geotechnical Engineering at the National Institute of Technology Rourkela is an authentic work carried out by him under our supervision and guidance. To the best of our knowledge, the matter embodied in the thesis has not been submitted to any other University/Institute for the award of any degree or diploma.

Place: Rourkela

Date:

Research Guide

Dr. S.P. Singh

Professor

National Institute of Technology

Rourkela

ACKNOWLEDGEMENT

First and foremost, I am glad and thankful to God for the blessing that has given upon me in all my endeavours.

I am deeply indebted to Dr. S.P. Singh Professor of Geotechnical Engineering specialization, my supervisor, for the motivation, guidance and patience throughout the research work. I appreciate his broad range of expertise and attention to detail, as well as the constant encouragement he has given me over the years.

I am grateful to Prof. N Roy, for his valuable suggestions during the synopsis meeting and necessary facilities for the research work. And also I am sincerely thankful to Prof. C.R. Patra, Prof. S.K.Das, Prof.R.K.Bag, Prof, Shantanu Patra and Prof. Ravi Behera for their kind cooperation and necessary advice.

I would like to thank my parents and family members. Without their love, patience and support, I could not have completed this work. Finally, I wish to thank co-workers of Geotechnical lab specially Narayan Mohanty and Dilip Das. I would like to thank many friends especially Shakti, Ram, Narsingh, Ali, Priyanka, Suryaleen and Swaraj for giving me support and encouragement during these difficult years.

ABHISHEK TIWARI

Table of Contents

List of figures	iii
List of tables	vi
Abstract	vii
CHAPTER-1 INTRODUCTION	
1.1 Introduction	1
1.2 Major Problems Caused by Shrinkage and Cracking	2
1.3 Advantages or Benefits of Image Analysis.....	3
1.4 Objective.....	4
CHAPTER-2 LITERATURE REVIEW AND SCOPE OF THE WORK	
2.1 Introduction	5
2.2 Literatures on Image Analysis	5
2.3 Literatures on Effect of Fly Ash in Synthetic Soil.....	7
2.4 Literatures on Effect of Reinforcement in Synthetic Soils.....	8
2.5 Literatures on Effect of Cracks and Shrinkage in Soils.....	11
CHAPTER-3 MATERIALS AND METHODOLOGY	
3.1 Introduction	9
3.2 Materials Used	9
3.2.1 Bentonite	9
3.2.2 Fly Ash	10
3.2.3 Recron, 3s, 6mm	11
3.3 Determination of Geotechnical Properties.....	11
3.3.1 Determination of Specific Gravity	11
3.3.2 Determination of Shrinkage Limit.....	12
3.3.3 Determination of Plastic Limit.....	12
3.3.4 Determination of Liquid Limit.....	13

3.3.5 Determination of Plasticity Index.....	14
3.3.6 Determination of Compaction Characteristics.....	14
3.4 Determination of Cracks Area and Shrinkage Area	15
3.4.1 Experimental Set-up	15
3.4.2 Specimen Preparation	17

CHAPTER-4 IMAGE ANALYSIS TECHNIQUE

4.1 Introduction.....	19
4.2 Image Processing	19
4.3 Image Analysis	21

CHAPTER-5 RESULTS AND DISCUSSION

5.1 General	26
5.2 Geotechnical Properties	26
5.2.1 Specific Gravity	26
5.2.2 Shrinkage Limit	27
5.2.3 Plastic Limit.....	27
5.2.4 Liquid Limit.....	28
5.2.5 Plasticity Index.....	28
5.2.6 Compaction characteristics	28
5.3 Determination of cracking and shrinkage behaviour.....	30
5.3.1 Without Fibres	30
5.3.2 Crack Length and Average Width of Cracks in Unreinforced Soil.....	47
5.3.3 With 2% recron 3s, 6mm fibres	48

CHAPTER-6 CONCLUSIONS

6.1 Summary... ..	53
6.2 Conclusions.	53
6.3 Future Work.	54

Table of Figures

Title	Page No
Fig 3.1 Experimental set up for taking the image of specimen	16
Fig 3.2 Sample mould of dia 13cm and thickness 5cm.....	18
Fig 3.3 Sample images of specimens prepared.....	18
Fig.4.1 Flow chart of the image processing method.....	20
Fig.4.2 Example of image processing and analysis.....	22
Fig 5.1 Variation of specific gravity and MDD with fly ash content	26
Fig 5.2 Variation of SL, PL and OMC with fly ash content.....	27
Fig 5.3 Variation of liquid limit and plasticity index with fly ash content.....	28
Fig 5.4 Proctor results (dry density vs moisture content)	29
Fig 5.4 a Variation of MDD with fly ash content.....	29
Fig 5.5 Variation of CDF with Fly Ash Content at LL for all the Specimen Thicknesses.....	30
Fig5.6 Variation of CDF with Fly Ash Content at PL for all the Specimen Thicknesses.....	30
Fig 5.7 Variation of CDF with fly ash content at OMC for all the specimen thickness.....	31
Fig 5.8 Variation of CDF with mc and thickness at 10% fly ash.....	31
Fig 5.9 Variation of CDF with mc and thickness at 20% fly ash.....	32
Fig 5.10 Variation of CDF with mc and thickness at 30% fly ash.....	32
Fig 5.11 Variation of CDF with mc and thickness at 40% fly ash	32
Fig 5.12 Variation of CDF with mc and thickness at 50% fly ash.....	33
Fig 5.13 Variation of CDF with mc and thickness at 60% fly ash.....	33
Fig 5.14 Variation of CDF with mc and thickness at 70% fly ash.....	33
Fig 5.15 Variation of CDF with mc and thickness at 80% fly ash.....	34
Fig 5.16 Variation of CDF with mc and thickness at 90% fly ash.....	34

Fig 5.17 Variation of CIF with fly ash content at LL for all the specimen thickness	35
Fig 5.18 variation of CIF with fly ash content at PL for all the specimen thickness.....	35
Fig 5.19 Variation of CIF with fly ash content at OMC for all the specimen thickness.....	35
Fig 5.20 variation of CIF with mc and specimen thickness at 10% FA.....	36
Fig 5.21 Variation of CIF with mc and specimen thickness at 20% FA.....	36
Fig 5.22 Variation of CIF with mc and specimen thickness at 30% FA.....	37
Fig 5.23 Variation of CIF with mc and specimen thickness at 40% FA.....	37
Fig 5.24 Variation of CIF with mc and specimen thickness at 50% FA.....	37
Fig 5.25 Variation of CIF with mc and specimen thickness at 60% FA.....	37
Fig 5.26 Variation of CIF with mc and specimen thickness at 70% FA.....	37
Fig 5.27 Variation of cracks area with fly ash content at LL for all the specimen thickness....	39
Fig 5.28 Variation of cracks area with fly ash content at PL for all the specimen thickness ...	39
Fig 5.29 Variation of cracks area with fly ash content at OMC for all the specimen thickness..	39
Fig 5.30 Variations in cracked area with moisture content and specimen thickness (cm) at 10% FA content.....	40
Fig 5.31 Variations in cracked area with moisture content and specimen thickness (cm) at 20% FA content.....	40
Fig 5.32 Variations in cracked area with moisture content and specimen thickness (cm) at 30% FA content.....	41
Fig 5.33 Variations in cracked area with moisture content and specimen thickness (cm) at 40% FA content	41
Fig 5.34 Variations in cracked area with moisture content and specimen thickness (cm) at 50% FA content.....	41
Fig 5.35 Variations in cracked area with moisture content and specimen thickness (cm) at 60% FA content.....	42

Fig 5.36 Variations in cracked area with moisture content and specimen thickness (cm) at 70% FA content	42
Fig 5.37 Variation of shrinkage area with fly ash content at LL for all the specimen thickness.	43
Fig 5.38 Variation of shrinkage area with fly ash content at PL for all the specimen thickness	43
Fig 5.39 Variation of shrinkage area with fly ash content at OMC for all the specimen thickness	43
Fig 5.40 Variation of shrinkage area with specimen thickness and moisture content at 10% fly ash content.....	44
Fig 5.41 Variation of shrinkage area with specimen thickness and moisture content at 20% fly ash content.....	44
Fig 5.42 Variation of shrinkage area with specimen thickness and moisture content at 30% fly ash content.....	44
Fig 5.43 Variation of shrinkage area with specimen thickness and moisture content at 40% fly ash content.....	45
Fig 5.44 Variation of shrinkage area with specimen thickness and moisture content at 50% fly ash content.....	45
Fig 5.45 Variation of shrinkage area with specimen thickness and moisture content at 60% fly ash content.....	45
Fig 5.46 Variation of shrinkage area with specimen thickness and moisture content at 70% fly ash content.....	46
Fig 5.47 Variation of shrinkage area with specimen thickness and moisture content at 80% fly ash content.....	46
Fig 5.48 Variation of shrinkage area with specimen thickness and moisture content at 90% fly ash content.....	46

List of Tables

Title	Page No
Table 3.1 Geotechnical Properties of Bentonite.....	9
Table 3.2 IS Classification of Soil.....	10
Table 3.3 Geotechnical Properties of Fly Ash.....	10
Table 3.4 Specific Gravity of B/F Mixes.....	11
Table 3.5 Shrinkage Limit of B/F Mixes.....	12
Table 3.6 Plastic Limit of B/F Mixes.....	13
Table 3.7 Liquid Limit of B/F Mixes.....	13
Table 3.8 Plasticity Index of B/F Mixes.....	14
Table 3.9 OMC and MDD for B/F Mixes.....	15
Table 3.10 Camera Features and Image Description.....	16
Table 5.1 Results of Total Cracks Length and Average Cracks Width of Unreinforced Soil	47
Table 5.2 Comparison of CDF for Reinforced and Unreinforced Soil.....	48

ABSTRACT

Surface cracks and shrinkage in soil affects its geotechnical properties in various ways. Permeability of soil changes due to cracks in clay barriers which lead to development of preferential flow paths for transportation of contaminants. Development of cracks may also lead to decrease in bearing capacity of soil. In case of earth embankments, cracks reduce strength and lead to seepage and percolation problems. Integrity and stability of landfill liners are affected by surface cracks, apart from leachate infiltration. Alignment of embedded pipes can be changed due to the surface shrinkage. They can cause slope instability and can contribute to the land slides in hilly areas. Hence, knowledge of surface cracks and the shrinkage behaviour of soil is essential to improve the understanding and prediction of changes of unsaturated hydraulic properties in heterogeneous and non-rigid soils. This paper is an attempt to introduce a novel methodology for quantifying surface cracks and shrinkage that appears in soil after desiccation under atmospheric conditions using image analysis technique. ImajeJ software has been used for image processing and Matlab for the calculation of surface cracks and shrinkage area. The samples used for the study is synthetic soil obtained by mixing bentonite and fly ash in various proportions. The effect of variable parameters like sample thickness, moisture content, fly ash content and fibres content on the surface cracks and shrinkage of the bentonite-fly ash mix have been studied. From results it was found that CDF and CIF depends on the chosen parameters i.e. fly ash content, moisture content, fibres content and specimen thickness. There was a reduction in CDF and CIF values with increase in fly ash content and fibres content, while it was increased with the increase in moisture content and specimen thickness.

1.1 Introduction

Expansive soils are highly sensitive to moisture content and temperature and generally undergo large volume changes when exposed to them. They swell when water content and temperature of soil increases and shrinks when the reduction in water content and temperature occurs. Bentonite soils and black cotton soils with a high content of expansive minerals like montmorillonite and smectite shows the most dramatic shrink-swell behaviour. They form deep and wide cracks with very high soil mass density in drier seasons, while in rainy season the cracks disappeared due to their self-healing tendency with very low soil mass density as they increase their volume manifolds.

Shrinkage is a process of densifying soil under capillary pressure. Volume reduction occurs as long as capillary forces are larger than the internal stresses that can be generated by soil. Sometimes, if the clay soils are dried from saturated state, they achieve such a high densities that cannot even be obtained by any general compacting method in the laboratory. This shows how enormous the pressures that generated during shrinkage process are! Shrinkage limit is the indicative of shrinkage potential of soil. Lower shrinkage limit value indicates higher shrinkage potential while higher value indicates lower shrinkage potential of the soil.

During acute shortage of rainfall the horizontal shrinkages are accompanied with the desiccation cracks. Cracks are the consequences of shrinkage that occurs due to the removal of pore water from soil. It is a complex phenomenon which occurs in most of the heterogeneous and non-rigid soils. They are initiated when the tensile stresses exceed the tensile strength of soil. Cracks density and intensity generally increases with the increase in thickness of a given soil specimen. Cracks and shrinkage depend on so many factors like percentage of clay in the soil, type of clay minerals, degree of weathering, initial moisture content, temperature, and specific surface area of clay particles, particle arrangement and thickness of deposition.

Cracks and shrinkage in soil affects its geotechnical properties in various ways. Permeability of soil changes due to cracks in clay barriers which lead to development of preferential flow paths for transportation of contaminants. Development of cracks may also

lead to decrease in bearing capacity of soil as a result of which non-uniform and differential settlement of foundation takes place. Apart from the leachate infiltrations, cracking may also affect the integrity and stability of landfill liners and covers. In case of earth embankments, cracks reduce strength and lead to seepage and percolation problems. Alignment of embedded pipes can be changed due to the surface shrinkage. They can cause slope instability and can contribute to the land slides in hilly areas. Hence, knowledge of surface cracks in soil and the shrinkage behaviour is essential to improve the understanding and prediction of changes of unsaturated hydraulic properties in heterogeneous and non-rigid soils.

This paper presents a novel methodology for the quantification of surface cracks and shrinkage by taking digital photographs of the specimen and then using the software ImageJ for image processing and Matlab for the calculations of cracks and shrinkage area. Synthetic soil prepared by mixing bentonite and fly ash in different proportions were used for the study. Fly ash content in the mix was varied from 10%, 20%, 30%.....to 90%. Specimen tested for experiments were prepared at liquid limit, plastic limit and at OMC and at three different thicknesses 5cm, 2.5cm and 1.5 cm. Later 2% recron©3s, 6mm fibres by weight of mix were also added in the specimen to further reduce the cracks. The effect of variable parameters like sample thickness, moisture content, fly ash content and fibres content on the surface cracks and shrinkage of the synthetic soil have been studied and reported.

1.2 Major Problems Caused by Shrinkage and Cracking

Cracking and shrinkage are always a headache to the civil engineers whether they are geotechnical engineers, transportation engineers, structural engineers, mining engineers, geological engineers or agricultural engineers. They can cause heavy disaster to the civil engineering structures in many ways. Some of the major problems that can be caused by the cracks and shrinkage are listed below:

1. In case of water canals, cracking increases the water loss through cracked surface area. Thus increases the cost of irrigation.
2. Cracking under foundation soil can cause differential settlement to the foundation. It increases the risk of structure failure.
3. In case of concrete work, cracks can provide way for the reactive chemicals to enter the concrete and thus creating the risk of its deterioration.

4. Water can seeps through the cracks developed on dam. Over a period of time they can create piping problem to the dam.
5. It can affect the stability and integrity of landfill liners, apart from the leachate infiltration.
6. They can create cracked driveways and pathways, thus making pavements maintenance difficult.
7. In rainy season expansive soil swell while in drought season they shrink with deep and wide cracks in it. These shrinkage and cracks make the root and stem of small plants and weeds to move from their original place and thus making them very weak.
8. In mine waste deposits, it can contributes to the contamination of surface and sub-surface water resources.
9. They can cause slope instability and can contributes to the land slides in hilly areas.
10. They can change the alignment of water pipes embedded in soil.

1.3 Advantages or Benefits of Image Analysis Technique

As the damage caused by cracking and shrinkage of soil is severe, therefore its accurate and precise quantification is a major challenge in front of civil engineers. For last so many year studies have been going on for the precise prediction of cracks and its parameters. Out of all the available methods image analysis is the best method because of its following advantages:

1. It is comparatively faster method and takes less time for quantifying cracks and shrinkage.
2. It is highly accurate and precise method. The cracked and shrinkage area obtained are generally more than the manually measured values as it also accounts the micro and hair cracks.
3. It does not depend on the shape and size of the specimen on the surface of which cracks and shrinkage are to be quantified.
4. Its results are also free from the constituent of the cracked materials.
5. Less number of labours are required.

6. This method is quite cheap as it requires only images and a software ImageJ which is freely available.
7. It is a non- destructive method and useful information can be obtained without touching the soil.
8. Its practical implication on the field is very easy.

1.4 Objective

Main objective of the research work is the quantification of cracks and shrinkage using image analysis technique. The effect of variable parameters like fly ash content, specimen thickness, fibres content and moisture content on the cracking and shrinkage behaviour of bentonite-fly ash mixes will be displayed.

2.1 Introduction:

Image analysis is not new in geotechnical engineering, but the advancement in the computer hardware and software capabilities has made it a new and efficient tool that can be automated and applied to a series of images without considering shape, size and constituent of the material. Some of the important literatures available on the image analysis are listed below.

2.2 Literatures on Image Analysis:

Lakshmikantha et al. conducted experiment on Barcelona silty clay. They prepared rectangular specimen of different areas with two thicknesses 10 mm and 20 mm. Image analysis was used to quantify the cracks. They observed the result for 10 mm and 20 mm thickness of specimen and found that the peaks of the distributions of the crack intersection angles are in the range between 90° and 120°. Depending on the existing stress conditions the intersecting cracks may form a “Y” or “T” joint, resulting in an intersection angle that varies between 90° for orthogonal cracks and 120° for non-orthogonal cracks. Most of the cracks angle lies between 80-100 degrees suggests the cracks were formed more by a tensile stresses. Evolution of cracks were shown by a series of images taken during the experiment. They also proposed that the CDF depends on the specimen thickness. Average CDF for 10-mm-thick specimens was found to be (CDF10) 10.2 % ($s=1.77$, standard deviation), whereas for the 20-mm-thick specimens it was (CDF20) 13 % ($s=1.08$).

Auvray et al. used mix containing 40% Xeuilley silt and 60% bentonite by weight to conduct their experiment. The materials were initially dried and sieved to 400 μm and then mixed together. They carried out their study to quantify the evolution of CIF and volumetric shrinkage in a clayey specimen submitted to suction-controlled drying-wetting cycles at a constant temperature of 20 °C by the help of ImageJ software.

They found the presence of cracks did not influence the relationship between the vertical strains and the suction cycle. The hysteresis loops corresponding to the vertical and radial strains are narrow whereas the CIF/ loops are large. Moreover, the comparison of the evolution of CIF(tot) and CIF/ with the mass water content showed that the main parts of the hysteresis loops were linked to the inner crack formation. The difference between these two curves mainly corresponds to the plastic volumetric deformation accumulated during the

first drying phase. The first cycle was the most influential. Here CIF means crack intensity factor and is given by the equation

$$\text{CIF}^* = \frac{\text{Crack area}}{\text{Reduced specimen area}} \times 100$$
$$\text{CIF}_{\text{tot}} = \frac{\text{Crack area} + \text{Shrinkage area}}{\text{Initial specimen area}} \times 100$$

Peng et al. carried out experiment on soil surface for the quantification of soil shrinkage in 2D by digital image processing. Soil surface showing the cracks, within the soil volume and surrounding the soil core between the soil and the cylinder wall, were photographed with a Sonny digital camera under macro model, positioned at a constant distance of 15 cm above the soil surface. Undisturbed soil cores (10 cm in diameter and 6.1 cm in height, three replicates) were taken by the stainless steel cylinder with the wall of 0.15 cm width. The field water content of the investigated soils reaches 89.0–93.2% of saturation.

They prepared images by the help of photoshop and and scion softwares. After verifying the results they found that the the image processing technique is highly accurate and it varies only by 1% with the manually calculated value of shrinkage. They stated this method to be inexpensive, non-destructive and even quick enough in quantifying any type of shrinkage.

Puppala et al. used Digital Imaging Technology for the measurement of volumetric shrinkage strain in expansive soils. The experimental program was designed to test four types of untreated and treated expansive soils to measure volumetric shrinkage strains by both conventional manual and digital image based measurements. The soils tested consist of two artificial lean clay soils with Kaolinite and Illite as the dominating clay minerals, and two natural fat clays rich in Montomorillonite clay mineral. All four soils were compacted as per standard Proctor test. Soil specimens were prepared at three different moisture content levels, namely liquid limit, plastic limit, and wet-of-optimum moisture content corresponding to 95% of maximum dry unit weight. Scion software was very much used to process all the photographs.

After final result they concluded that the Digital analysis provided higher volumetric shrinkage strains than manual measurements since irregular and hairline cracks in the soils were taken into account, thereby providing more precise estimation of shrinkage strain potentials of expansive soils. An increase in compaction moisture contents in soils resulted in increased shrinkage.

B. F. Lim and G. A. Siemens presented an unconfined swelling test apparatus and methodology for measuring the maximum swelling deformation of a soil under true free stress conditions. The methodology includes a non-contact method using digital image analysis to measure deformations. The in-test results indicate that primary and secondary swelling behaviour and anisotropic swelling can be measured using the employed non-contact deformation method. The soil swelling deformation calculated with GeoPIV analysis is also in general agreement with end-of-test measurements. The effect of the AR on the swelling behaviour is noted regarding the initial swelling rate and the time needed to reach equilibrium with the applied wetting conditions. The end-of-test measurements shows consistent behaviour for the specimens tested and that a high degree of saturation was achieved during the test. The maximum swelling deformation for Bear paw soil is in the range of 60 % to 70 % volumetric strain under unconfined swelling conditions. The results were interpreted in the Swell Equilibrium Limit framework to allow analysis and prediction of swelling soil deformations. This extends the use of the Swell Equilibrium Limit framework down to nominal stress levels.

2.3 Literatures on Effect of Fly Ash in Synthetic Soils:

Bidula Bose conducted experiments on Sodium bentonite and fly ash obtained from Rourkela Steel Plant to examine the effect of addition of fly ash on the geotechnical behaviour of the expansive soil in terms of grain size distribution, Atterberg limits, specific gravity, compaction characteristics, free swell, swell potential, swelling pressure, axial shrinkage percent, and unconfined compressive strength as per IS code. He mixed the sodium bentonite with various proportions of fly ash ranging from 0, 20, 40, 60, 80 and 90 percentages. He found liquid limit, plastic limit, plasticity index, linear shrinkage swelling pressure, free swell index (FSI) decreases while shrinkage limit and OMC increases with increase in fly ash content. MDD increases upto 20% of fly ash and then gradually decreases with the increase in fly ash content.

B.A. Mir used high-calcium and low-calcium fly ashes to investigate the effect of fly ash on the swelling potential of black cotton soil. From the study he concluded that FSI, swelling potential, swelling pressure and MDD decreases while, OMC and shrinkage limit increases with the addition of fly ash.

2.4 Literatures on Effect of Reinforcement in Synthetic Soils:

Arpan Laskar and Sujit Kumar Pal conducted study on two types of soil locally found in Tripura. For reinforcement HDPE waste plastic bottle fibres were used. They found that with increase in HDPE fibre content MDD decreases. Compression index (C_c) & coeff of volume change (m_v) decreases upto 0.50% fibre content. Value increases with further inclusion of fibres 1% in soil. OMC is independent of amount of HDPE fibres, as it do not absorb water. Value of coefficient of consolidation increases with the increase in plastic fibres.

Azadegan et al. conducted their studies on a clayey soil with Ferrous Kaolinite minerals of west Kerman's surface clay. He used randomly distributed palm fibres of 30mm size in clayey soils. He found that with increase in palm fibre ratio more volume change would occur as the palm fibres being a product from natural woods absorb water very fast and carry it through the length of fibres like a conducting pipe. But after the shrinkage procedure ends crack revised from deep, wide and long ones to completely distributed cracks with the increment in fibres ratio. However mechanical properties of the reinforced soil like elasticity modulus, compressive strength and the ultimate strain increases when more fibres were applied.

Amit Shrivastava et al. used different percentages of shredded tyre waste to reinforce black cotton soil with two different categories fine (passing 2.0–0.075 mm retained) and coarse (passing 4.75–2.0 mm retained) He found 30–50% addition of shredded tyre waste in expansive black cotton soil reduces the volume change potential and shearing strength. Addition of 5% shredded tyre waste in black cotton soil will provide a mix having a lighter weight and marginally improved shear strength. Addition of coarse shredded tyre waste increases the consolidation properties that may be attributed to the increased permeability values of the mix. It also increases the compressibility properties of the mix.

Maheri et al. conducted a series of tests on samples made of different material mixes to determine the effects of lime and crusher dust on the strength and durability of the improved kahghel plaster by considering three particular problem variables clay and crusher dust contents, lime content and straw content. He suggested an optimum mix design, indicate that additions, by weight of the dry mix, of 10% hydrated lime, 10% crusher dust and 2% crushed straw fibres to a high clay content soil with plasticity index $PI \geq 30$, produces the desired clay plaster.

CHAPTER 3

MATERIALS AND METHODOLOGY

3.1 Introduction

Sodium bentonite clay is highly expansive soil and is very much prone to large volume changes (swelling and shrinkage) that are directly related to change in water content. This experimental set-up makes it possible for us to quantify cracks and shrinkage in virgin bentonite clay and to study the impact of some of the parameters that affect the intensity and density of cracks. These cracks and shrinkage were reduced by increasing the fly ash content and introducing fibres in the mix and by reducing the moisture content and specimen thickness.

3.2 Materials used

Experimental work has been carried out by mixing bentonite and fly ash in different proportions with distilled water at three different moisture content i.e. at OMC, plastic limit and at liquid limit. The various proportions of fly ash used in mixtures were 10%, 20%, 30%, 40%, 50%, 60%, 70%, 80% and 90% by weight. These mixes were used to prepare specimens of three different thicknesses 5cm, 2.5cm and 1.5cm. The materials were initially oven dried and sieved to 425 μm before mixing with distilled water. Prepared specimens were dried and then photographed. Later image processing and analysis is done by using image analysis technique. Fibres were also added in the mix to further reduce the surface shrinkage.

3.2.1 Bentonite

The soil used in the experiment is commercially available sodium bentonite clay having 13.15% natural moisture content. It was sieved through 425 microns sieve and is oven dried before its use. It is then kept in an air-tight container for subsequent use. The geotechnical properties of the bentonite is summarised in table 3.1 below:

Table 3.1 Geotechnical Properties of Bentonite

Shrinkage Limit	5.11 %
Plastic Limit	50.20 %

Liquid Limit	301 %
Plasticity Index	250.79 %
Specific Gravity	2.7
OMC	32 %
MDD	1.38 g/cc

According to the IS classification of soil system (table-3.2), it can be classified as high plasticity clay as plasticity index of bentonite is more than 50%

Table 3.2 IS Classification of Soil

Low Plasticity	WL < 35%
Intermediate plasticity	WL < 35% < 50%
High plasticity	WL > 50%

3.2.2 Fly Ash

Fly ash used in the study is collected from Rourkela Steel Plant, Odisha. It was of light grey in colour and having 88% silt and clay and 12% fine sand when sieved through 2mm sieve. It has 1.1% natural moisture content. It can be classified as non-plastic. The sample was oven dried at the temperature 105-110°C and then sieved through 425 microns sieve before its use. The basic geotechnical properties of fly ash is given in table 3.3 below. The fly ash samples were stored in airtight container for subsequent use.

Table 3.3 Geotechnical Properties of Fly Ash

Shrinkage Limit	41.52 %
Plastic Limit	NP
Liquid Limit	51.6 %
Plasticity Index	NP
Specific Gravity	2.3

OMC	40 %
MDD	1.16

* NP = Non-Plastic

3.2.3 Recron© 3s, 6mm fibres

Recron© 3s, a product of Reliance Industries Limited, is the New Generation “Secondary Reinforcement” for construction industries. For the present study fibres having melting point 250°C and length 6 mm were used. Only 2% of fibre content was used in the bentonite-fly ash mix.

3.3 Determination of Geotechnical Properties

3.3.1 Determination of Specific Gravity

The specific gravity of bentonite, fly ash and their mixes in different proportions were determined by using Le-Chatelier flask with Kerosene as the solvent as per IS: 2720 (Part-III, section-1) 1980. The specific gravity of bentonite and fly ash were found to be 2.7 and 2.3 respectively. Specific gravity for bentonite-fly ash mixes are presented below.

Table 3.4 Specific Gravity of B/F Mixes

Fly ash and bentonite percentage in the mix	Specific Gravity
FA 0, BT 100	2.7
FA 10, BT 90	2.64
FA 20, BT 80	2.59
FA 30, BT 70	2.57
FA 40, BT 60	2.55
FA 50, BT 50	2.53
FA 60, BT 40	2.51
FA 70, BT 30	2.48
FA 80, BT 20	2.43
FA 90, BT 10	2.36
FA 100, BT 00	2.3

*FA = Fly Ash and BT= Bentonite

3.3.2 Determination of Shrinkage Limit

This test was performed to determine the shrinkage potential of bentonite, fly ash and their mixes. Low value of shrinkage limit means the soil has high shrinkage potential and vice versa. Shrinkage limit is the moisture content below which no reduction in volume takes place even after the reduction in moisture content of the soil. Fly ash and bentonite were oven dried and sieved through 425 microns size sieve before mixing it with distilled water at moisture content more than the expected shrinkage limit. Mixes were kept in air tight polythene bags for 48 hours to homogenise the water content. Shrinkage limit is then determined as per the IS: 2720 (Part 6) guidelines. Shrinkage limit of bentonite was found to be 5.11% and for fly ash it was 41.52. For bentonite-fly ash mixes shrinkage limits are given in table 3.5

Table 3.5 Shrinkage Limit of B/F Mixes

Fly ash and bentonite percentage in the mix	Shrinkage Limit (%)
FA 0, BT 100	2.11
FA 10, BT 90	5.94
FA 20, BT 80	7.73
FA 30, BT 70	15.44
FA 40, BT 60	22.53
FA 50, BT 50	26.22
FA 60, BT 40	34.61
FA 70, BT 30	35.86
FA 80, BT 20	36.3
FA 90, BT 10	38.04
FA 100, BT 00	41.52

**FA = Fly Ash and BT= Bentonite*

3.3.3 Determination of Plastic Limit

This test was performed to determine the moisture content of the soil below which soil starts to lose its plasticity. For any soil it is determined by rolling a thread of 3 mm dia out of it and the moisture content when it starts crumbling will be the plastic limit of the soil. A material will be non-plastic if it is not possible to make a thread of dia 3mm at any moisture content. This test was performed as per IS: 2720 (Part 5) guidelines. Results of this test is stated below:

Table 3.6 Plastic Limit of B/F Mixes

Fly ash and bentonite percentage in the mix	Plastic Limit (%)
FA 0, BT 100	50.21
FA 10, BT 90	49.36
FA 20, BT 80	48.88
FA 30, BT 70	48.23
FA 40, BT 60	47.64
FA 50, BT 50	47.12
FA 60, BT 40	46.65
FA 70, BT 30	46.03
FA 80, BT 20	44.67
FA 90, BT 10	43.92
FA 100, BT 00	NP

**FA = Fly Ash and BT= Bentonite*

3.3.4 Determination of Liquid Limit

Liquid limit is the minimum moisture content above which the soil starts to behave as a liquid and loses all of its shear strength. Casagrande apparatus was used to determine the liquid limit of bentonite and bentonite mixes having fly ash content less than 80% while cone penetrometer is used to determine the liquid limit of fly ash and mix having 90% fly ash content as they are non-plastic and non-cohesive. IS: 2720 (Part 5) has been followed for the determination of liquid limit. Liquid limit for bentonite, fly ash and their mixes are shown below:

Table 3.7 Liquid Limit of B/F Mixes

Fly ash and bentonite percentage in the mix	Liquid Limit (%)
FA 0, BT 100	301
FA 10, BT 90	266
FA 20, BT 80	230
FA 30, BT 70	199
FA 40, BT 60	176
FA 50, BT 50	147
FA 60, BT 40	126
FA 70, BT 30	98

FA 80, BT 20	72
FA 90, BT 10	53
FA 100, BT 00	51.6

**FA = Fly Ash and BT= Bentonite*

3.3.5 Determination of Plasticity Index

Plasticity Index is the measure of water content up to which the soil shows plastic behaviour. It is calculated from the following relation

$$I_p = WL - W_p$$

Where, I_p = plasticity index in %,

WL = liquid limit in %

WP = plastic limit in %

For bentonite, fly ash and various mixes plasticity index was found as below:

Table 3.8 Plasticity Index of B/F Mixes

Fly ash and bentonite percentage in the mix	Plasticity Index (%)
FA 0, BT 100	250.79
FA 10, BT 90	216.64
FA 20, BT 80	181.12
FA 30, BT 70	150.77
FA 40, BT 60	128.36
FA 50, BT 50	99.88
FA 60, BT 40	79.35
FA 70, BT 30	51.97
FA 80, BT 20	27.33
FA 90, BT 10	9.08
FA 100, BT 00	NP

**FA = Fly Ash and BT= Bentonite*

3.3.6 Determination of Compaction Characteristics

The moisture content and dry density relationships for bentonite-fly ash mixes were found by using Proctor compaction tests as per IS: 2720 (Part VII) 1980. Mixes were thoroughly mixed with adequate amount of water and kept in air tight container for 48 hours to make it homogeneous. They were filled in three layers in Proctor mould and each layer was given

25 blows with a rammer of 2.6kg dropped from a height 31 cm. Maximum Dry Density and corresponding moisture content i.e. OMC can be found out from the plotted graph between dry density vs moisture content. OMC and MDD for different ratios of bentonite-fly ash mixes are given in table below:

Table 3.9 OMC and MDD for B/F Mixes

Fly ash and bentonite percentage in the mix	OMC (%)	MDD (g/cc)
FA 0, BT 100	32	1.38
FA 10, BT 90	31	1.39
FA 20, BT 80	30.5	1.41
FA 30, BT 70	30.5	1.4
FA 40, BT 60	30.5	1.395
FA 50, BT 50	31.4	1.39
FA 60, BT 40	31.6	1.37
FA 70, BT 30	33	1.34
FA 80, BT 20	34	1.315
FA 90, BT 10	36.2	1.25
FA 100, BT 00	40	1.16

**FA = Fly Ash and BT= Bentonite*

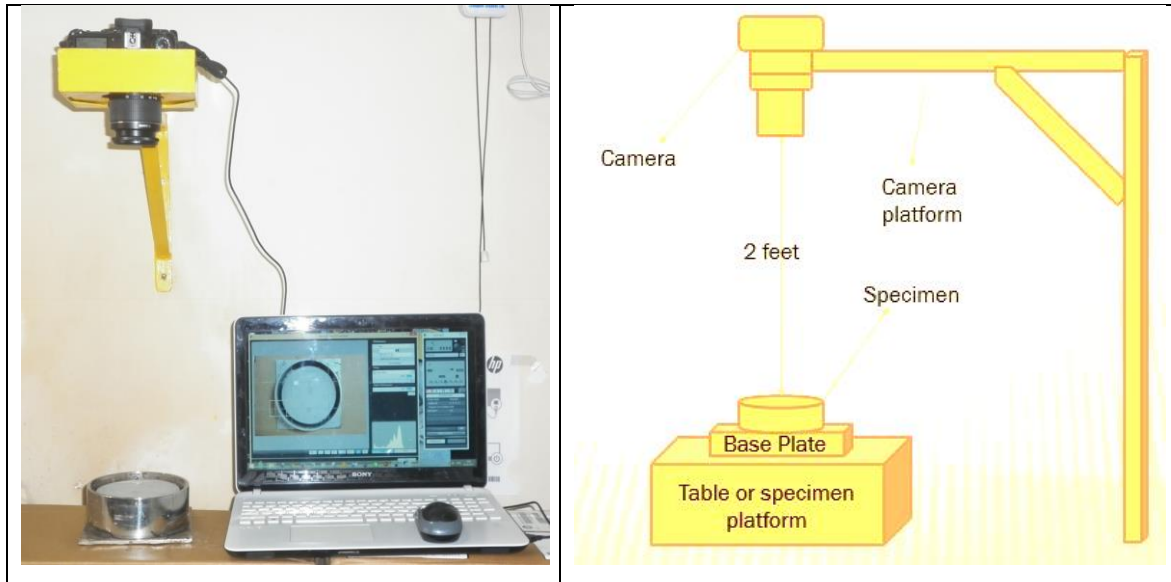
3.4 Determination of Cracks Area and Shrinkage Area

3.4.1 Experimental Set-up

A novel method was developed for the quantification of cracks and shrinkage in the laboratory. Specimen of 9 different proportions of bentonite-fly ash mixes (F10B90, F20B80, F30B70, F40B60, F50B50, F60B40, F70B30, F80B20 and F90B10) were prepared at three moisture content (OMC, plastic limit and liquid limit) and at three different thicknesses (5cm, 2.5cm and 1.5cm). For the preparation of specimen three moulds of mild steel with thin base plate having 13 cm dia and depth 5cm, 2.5cm and 1.5cm were used. Experimental set up includes a high resolution digital camera Canon EOS 60D and a platform to support camera at a fixed height of 2 feet from the specimen. Camera is connected to PC through data cable to facilitate an automated system to capture still photographs without disturbing the camera. The images obtained were processed in software

ImageJ and then the required information can easily be determined by using Matlab and Microsoft Excel.

Fig 3.1 Experimental set up for taking the image of specimen



Camera (Canon EOS 60D) used in the experiment and images taken by it have the following features:

Table 3.10 Camera Features and Image Description

IMAGES	
Dimension	5184 * 3456
Width	5184 pixels
Height	3456 pixels
Horizontal resolution	96 dpi
Vertical resolution	96 dpi
Bit depth	24
Compression	
Resolution unit	2
Color representation	sRGB
Compressed bits/pixel	
CAMERA	
Camera maker	Canon

Camera model	Canon EOS 60D
F-stop	f/5.6
Exposure time	1/100 sec
ISO speed	ISO-3200
Exposure bias	0 step
Focal length	55mm

3.4.2 Specimens Preparation:

Following procedure was adopted for the preparation of specimen:

1. Liquid limit, plastic limit and OMC for each ratios of bentonite-fly ash mixes were determined as per the guidelines given in codes. For liquid limit and plastic limit it is (IS: 2720-part 5) and OMC can be found out by Standard Proctor test (IS: 2720-part7).
2. Bentonite and fly ash were oven dried and mixed together with distilled water at the required proportion of bentonite-fly ash mix and at three moisture content OMC, LL and PL.
3. These mixes were kept in air-tight polythene bags for 48 hours to homogenise the water content without any loss of water due to evaporation. For reinforced specimen, 2% fibres by weight of mix is added at the time of mixing bentonite and fly ash and then they were kept for 48 hours
4. Specimens were prepared in the properly greased cylindrical mould of dia 13 cm and thicknesses 5cm, 2.5cm and 1.5cm. Inside of mould should be painted black while the outer of the mould should be painted white so that the inner and outer area of mould be clearly separated.
5. They were suitably compacted to the maximum density by means of hydraulic jack, piston and collar. After compaction collar was removed and specimen surface was levelled by using knife. Same procedure is followed for the preparation of each specimen.
6. All specimens were kept at room temperature (27°C) for drying at least for 7 days and then they were transferred to the oven at constant temperature of 100°C-105°C for 24 hours.

7. Specimens were brought to the setup where camera is placed in platform and is connected to a PC through data cable.
8. Plumb-bob is used to ensure that the camera is vertical to the specimen surface. Inclined camera can cause scale defect. Photographs were clicked by the camera from the constant height of 60cm.
9. Raw images obtained were then processed and analysed by using image analysis technique. ImageJ software is used for image processing and Matlab is used for the calculations.
10. Areas obtained in sq px can be used to find some other related meaningful data in Microsoft Excel.

Fig 3.2 Sample mould of dia 13cm and thickness 5cm



Fig 3.3 Sample Images of Specimens Prepared



4.1 Introduction

Extraction of meaningful information from digital images clicked by digital camera by means of image processing is known as image analysis. It is performed in two basic steps. The first step involves the image processing in which image is prepared in various stages for further analysis. This include the conversion of RGB image to a grey scale image, and then to a binary (black & white) image obtained by thresholding the grey scale image. The second step consists of the analysis of the processed image obtained from step 1 to calculate the parameters that characterize the crack and shrinkage patterns like total area of cracks, total length of cracks, cracks average width, length of cracks per unit area, shrinkage area, crack density factor (CDF) and cracks intensity factor (CIF).

Several binary operations has to be performed to carry out these operations. A flow diagram for the image analysis technique is shown in fig 4.1 below. After getting areas in sq pixels, these values can suitably be changed into sq cm or sq mm in the Microsoft Excel.

4.2 Image Processing

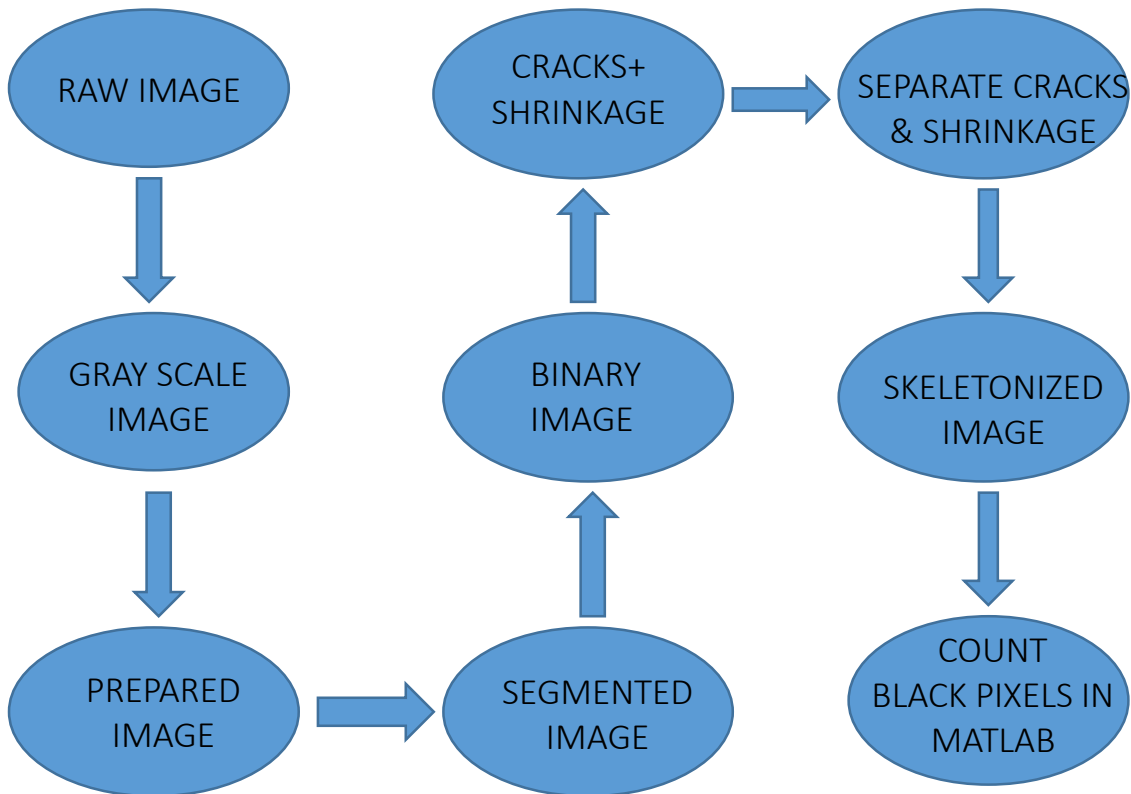
Process of changing a raw image into an improved image from which the desired information can be obtained is known as Image Processing. Image enhancement is done by increasing contrast, sharpness and adjusting brightness, saturation and colour. It can further be changed into binary images for edge separation. Some of the basic operations used in image processing are summarized below.

1. Preparation of the raw images

The picture taken by camera is an uncentred RGB (Red green Blue) image. In ImageJ software **circular crop** option can be used to crop any circular area. Preparation of image consists of selecting the inner circular area of mould and cropping the outer area to get a centred RGB image with white background. This image is then converted to 8-bit grey-scale image by going to the option in Imagej window **Image-type-8 bit**. A grey-scale image is the image in which the only colour are shades of grey. Three intensities are needed to specify each pixel in a full colour image A grey colour is the one in which the red, green and blue

components all have equal intensity in the RGB space and so it is only necessary to specify a single intensity for each pixel.

FIG 4.1 FLOW CHART OF THE IMAGE PROCESSING METHOD



2. Grey-Scale Processing

The images taken by the camera should not have any illumination on specimen surface otherwise it will affect the results. For its correction and to enhance the details of interest grey scale processing was performed. It is done in two single operations: (a) Subtract background that removes smooth continuous backgrounds (b) Un-sharpen mask that enhances and sharpens the edges of image by subtracting a blurred version of the image.

3. Image Segmentation

Image segmentation is done to separate the crack and shrinkage area from intact soil. It is done by thresholding the grey scale image with a fixed threshold value. In ImageJ it can be done by going to the option **Image-Adjust-Threshold**. Threshold value can be adjusted

manually if whole data is not there. It divides the whole image into multiple regions. Cracked and shrinkage area is having darker pixels as the light does not enter in them, while the surface area of intact soil is of lighter pixels because enough light falls on its surface. By thresholding all the pixels in images were changed to 0 a black pixel or 255 a white pixel by setting a threshold value. A pixel whose value is less than the threshold value will become black while those pixels whose value is more than the threshold value will become white.

4. Binary Processing

After segmentation if any error remains in the image like 'salt in pepper' in the cracks and shrinkage area or 'pepper in the salt' in the intact soil then it can be corrected by some basic binary operations. Go to **Process-Binary-Make binary** in ImageJ to perform further binary processing to the Images. **Erode** replaces each pixel with the minimum (lightest) value in a 3*3 neighbourhood. It is effective in removing pixels from the edges of black objects. **Dilate** replaces each pixel with the maximum (darkest) value in a 3*3 neighbourhood. It can effectively add pixels to the edges of black objects. **OPEN** performs an **ERODE** operation followed by a **DILATE** operation, smoothing objects and removing isolated pixels. **CLOSE** performs a **DILATE** operation followed by an **ERODE** operation, smoothing objects and filling in small holes. Some valuable data loss can be done by **Close** operation and hence it can be replaced by **Despeckle** median filter operation. This filter replaces each pixel with the median value in its 3*3 neighbourhood.

4.3 Image Analysis

It is done to calculate the desired data from the processed image.

1. Characterization of Cracks Pattern

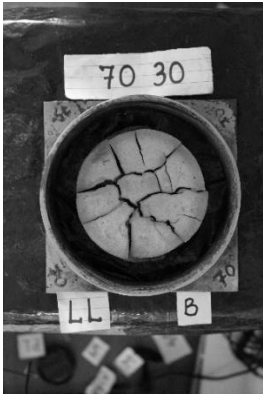
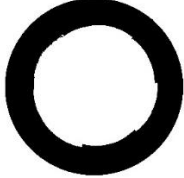
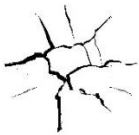
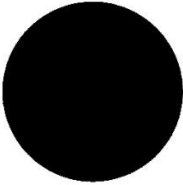
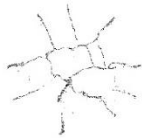
Processed image obtained by the operations performed from step 1 to step 4 on RGB image were then analysed in Matlab to gain some important information. Matlab program was written in such a way that it counts only the area of black pixels in the image. These black pixels shows the cracked area and shrinkage area. Shrinkage area and cracked area were separated from each other by using wand and cropping tool in ImageJ. Binary images were run in Matlab program to obtain results in sq px. These values are then converted to sq cm by using simple mathematics in Microsoft Excel.

For the determination of total length of cracks, some known distance in the image like the dia of mould is marked by straight line and scale is set in ImageJ by going to the option **Analyse - Set Scale – give value 13 cm**. In the same image the cracks from binary image is separated out and by using skeletonize command (**Process - Binary – Skeletonize**) the

cracks were changed into single pixel wide cracks along length. By going to **analyse – measure** command we get the total length of cracks in cm in perimeter column.

An example of image analysis for a specimen mix of 70% bentonite and 30% fly ash of 5cm thickness and at liquid limit is shown in the fig below:

Fig 4.2 Example of Image Processing and Analysis

<p>1.RAW IMAGE</p> 	<p>2.GREY SCALE IMAGE</p> 	<p>3.PREPARED IMAGE</p> 
<p>4.THRESHOLDING AND MAKING BINARY TO GET SEGMENTED IMAGE</p>	<p>5.SHRINKAGE+CRACKED</p> 	<p>6.SHRINKAGE AREA</p> 
<p>7.CRACKED AREA</p> 	<p>8.INITIAL SPECIMEN AREA</p> 	<p>9.SKELETONIZED</p> 

2. Calculations in Matlab and Microsoft Excel:

For the calculations of different parameters, following method was adopted. For illustration purpose a specimen from mix B70F30, of 5cm thickness and at liquid limit is selected and its calculations are shown below:

1. First the initial specimen area in sq px is calculated in Matlab by counting black pixels. For the given specimen it was 4928683 sq px.
2. Shrinkage area + crack area is then calculated for the same. It was 2712605 sq px.
3. Shrinkage area and cracked area is then calculated separately. (SA=2569145 sq px and CA= 143460 sq px.)
4. Reduced specimen area is calculated by subtracting shrinkage area from the whole specimen area. (RSA=2359538 sq px)
5. Shrinkage percentage is calculated by the following equations

$$\begin{aligned}\text{Shrinkage Area \%} &= \frac{\text{shrinkage area in sq px} \times 100}{\text{Initial specimen area in sq px}} \\ &= \frac{2569145 \times 100}{4928683} = 52.126\%\end{aligned}$$

6. Cracked percentage is calculated as below

$$\begin{aligned}\text{Crack area \%} &= \frac{\text{Cracked area in sq px} \times 100}{\text{Initial specimen area in sq px}} \\ &= \frac{143460 \times 100}{4928683} = 2.91\%\end{aligned}$$

7. CIF (Cracked Intensity Factor) is the percentage of cracks in reduced specimen area,

$$\begin{aligned}\text{CIF} &= \frac{\text{Cracked Area in sq px} \times 100}{\text{Reduced Specimen Area in sq px}} \\ &= \frac{143460 \times 100}{2359538} = 6.08\%\end{aligned}$$

8. CDF (Cracked Density Factor) is the percentage of total shrinkage and cracked area in the initial specimen area,

$$\begin{aligned} \text{CDF} &= \frac{\text{Shrinkage Area} + \text{Cracked Area in sq px} \times 100}{\text{Initial specimen area in sq px}} \\ &= \frac{(2569145 + 143460) \times 100}{4928683} = 55.037\% \end{aligned}$$

9. Now all the parameters Cracked Area, Shrinkage Area, CIF and CDF can be obtained in sq cm by multiplying their percentage to the area of mould i.e.

$$= \frac{\pi \times 13 \times 13}{4} = 132.732 \text{ sq cm}$$

Thus the crack area for the given sample will be = 2.91% of 132.732

$$= 0.0291 \times 132.732 = 3.86 \text{ sq cm}$$

And, the shrinkage area = 52.126% × 132.732

$$= 69.188 \text{ sq cm}$$

$$\text{CIF} = 6.08\% \times 132.732$$

$$= 8.07 \text{ sq cm}$$

$$\text{CDF} = 55.037\% \times 132.732$$

$$= 73.05 \text{ sq cm}$$

10. For finding the length of cracks, some known distance in the image like the dia of mould is marked by straight line and scale is set in ImageJ by going to the option **Analyse - Set Scale – give value 13 cm.**
11. In the same image the cracks from binary image is separated out and by using skeletonize command (**Process - Binary – Skeletonize**) the cracks were changed into single pixel wide image lengthwise.
12. **Analyse – Measure** command gave the value 38.691 cm.

13. Average width was calculated by dividing the crack area to the total length of cracks,

$$= \frac{3.86}{38.691} = 0.9976 \text{ mm}$$

14. Same procedure is repeated for each specimen.

RESULTS AND DISCUSSION

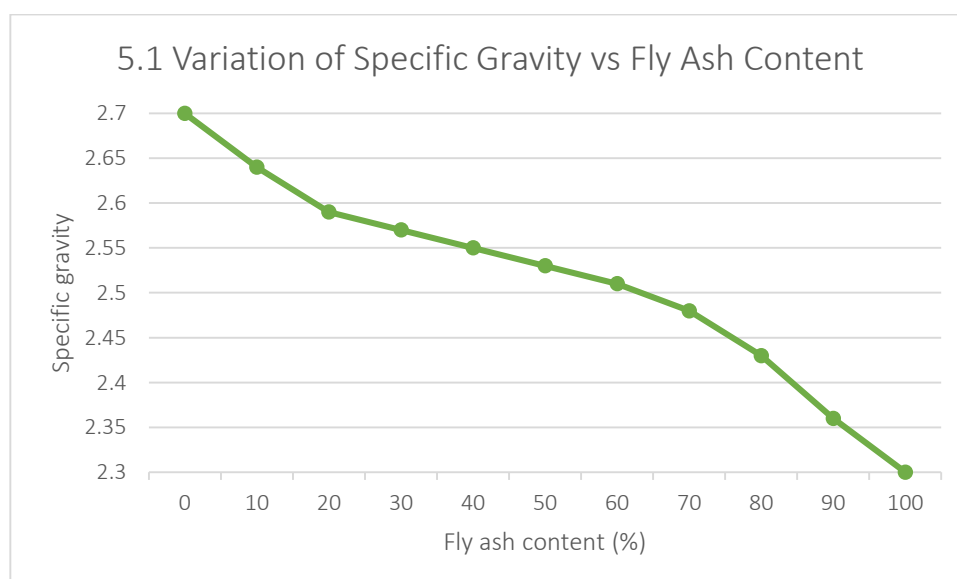
5.1 General

Addition of fly ash in highly expansive sodium bentonite soil has improved most of its geotechnical properties including cracking and shrinkage behaviour. Further reduction in cracking and shrinkage behaviour of reinforced bentonite-fly ash mix was observed when 2% recron©3s, 6mm fibres were added. Cracks revised from deep, wide and long ones to completely distributed cracks while the surface shrinkage area was reduced by 50-60% for most of the reinforced bentonite-fly ash mix. Hence fly ash addition with some fibres to the expansive soil is a good option for its stabilization and to improve its geotechnical properties.

5.2 Geotechnical Properties

5.2.1 Specific gravity

Specific gravity for bentonite, fly ash and bentonite-fly ash mixes were determined according to IS: 2720 (Part-III, section-1)1980. It was 2.7 for bentonite and 2.3 for fly ash. Either the presence of large number of hollow cenospheres from which the entrapped micro bubbles of air cannot be removed, or the variation in the chemical composition, particularly in iron content are the main cause of low specific gravity of fly ash. For mixes if the proportions of material with low specific gravity will increase then surely the overall specific gravity of mix will be reduced. These values reduced from 2.64 for 10% fly ash content to 2.36 for 90% fly ash content. Variation of specific gravity with fly ash content is shown in graph-5.1

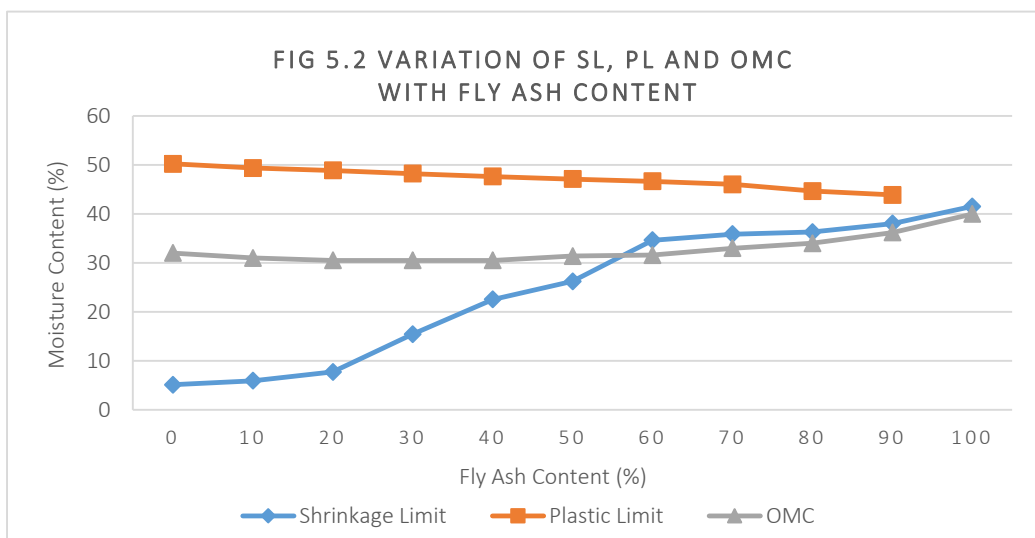


5.2.2 Shrinkage Limit

Shrinkage limit of bentonite-fly ash mixes were determined as per IS: 2720 (Part 6). Shrinkage limit of bentonite soil was very low as it contain so many free negatively charged clay particles which react with dipolar water molecule and adsorb a thick double layer of water on their surfaces. Montmorillonite present in bentonite even allowed more water to enter into unit layers. Having large specific area and highly charged particles, they can retain a very good amount of water in them. So they show very high shrinkage potential or low shrinkage limit. While fly ash are generally non-reactive. They adsorb a very thin layer of water and that also not for very long. Therefore the shrinkage potential of fly ash was very low and shrinkage limit is very high almost equal to its liquid limit. Increase in the percentage of non-shrinking fly ash in mixes thus increases the shrinkage limit and reduces its swelling potential. Variation of shrinkage limit with fly ash content in mixes is shown in fig-5.2

5.2.3 Plastic Limit

Because of the high percentage of clay minerals, bentonite shows good cohesive and plastic properties. In fly ash, these clay minerals are absent. Therefore it does not show any plastic behaviour. With increase in percentage of non-plastic material to a plastic material in mix, the plastic limit of mix will decrease and the same trend was obtained for bentonite-fly ash mixes. A comparison graph of plastic limit vs fly ash content is shown in fig-5.2

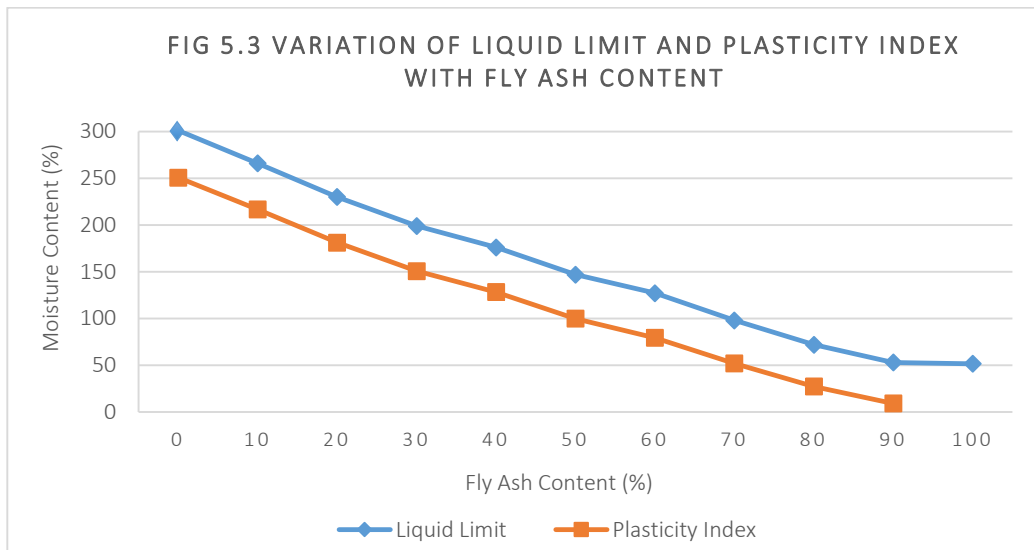


5.2.4 Liquid Limit

Liquid limit is that amount of water content that is needed just to satisfy the double layer of the clay particles. Bentonite clay particles have large surface area with highly negatively charged face so they can strongly held a thick layers of polar water. The amount of free water available is considerably low. So more water is required to satisfy double layer of water. Hence bentonite soil has very high liquid limit. But in case of fly ash, they contain very less charged particles. As a result of which a very thin layer of water can be held by the particles of fly ash. For the same mass of bentonite and fly ash free water available will be more for fly ash. Hence liquid limit for fly ash is very low as compared to bentonite. Liquid limit decreases with increase in fly ash content in the mix. Variation of liquid limit and fly ash content is shown in fig-5.3

5.2.5 Plasticity Index

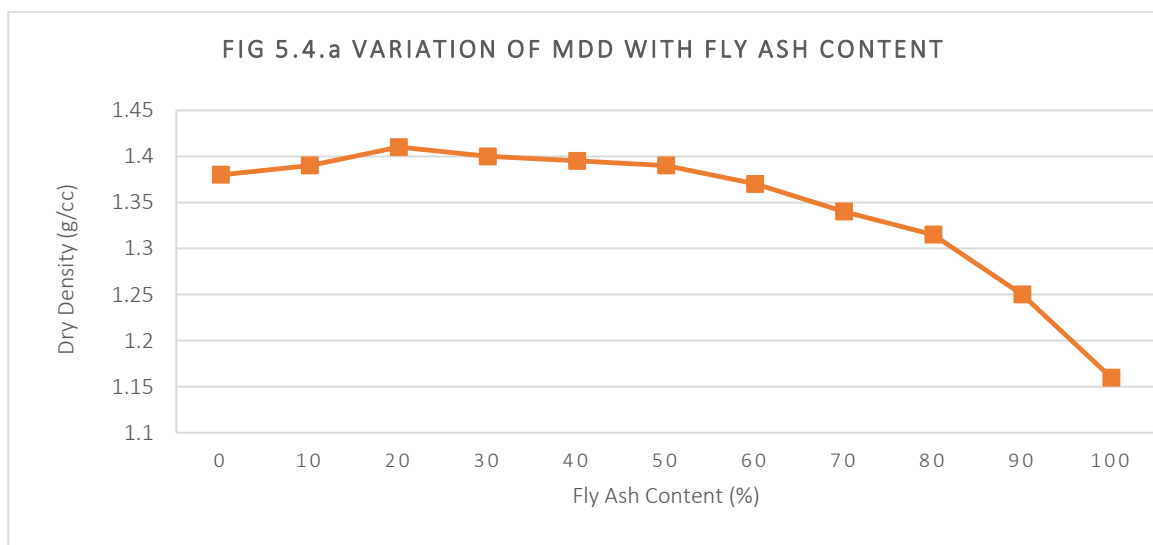
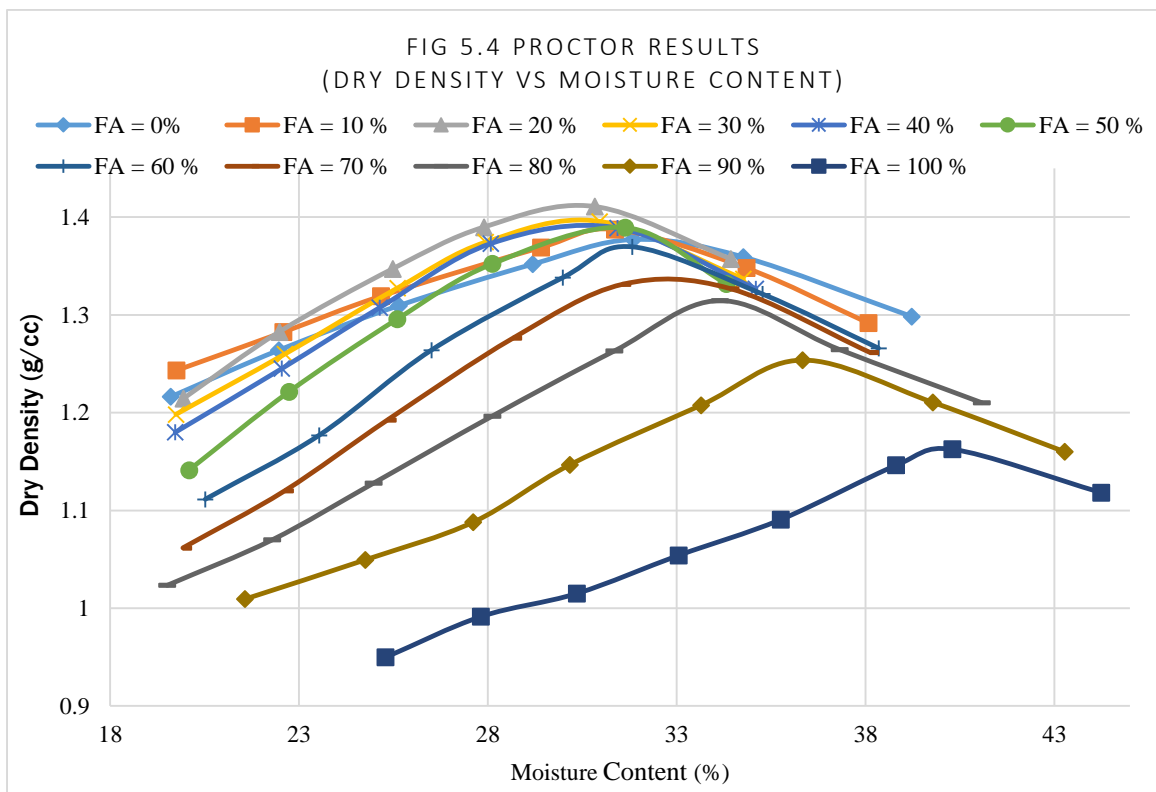
Plasticity index is the amount of water content loosely held by a clay particle in a double layer system. It is the measure of difference of liquid limit and plastic limit. Decrease in plasticity index was observed with the increase in fly ash content. Variation graph of plasticity index vs fly ash content is shown in fig-5.3



5.2.6 Compaction Characteristics

Proctor test results for bentonite, fly ash and mixes in different proportions are displayed in fig-5.4. From the graphs, OMC and MDD, the two compaction characteristics were determined for them. Initially OMC was decreasing with the increase in fly ash content upto 20% and then starts increasing. While just opposite behaviour is shown by the graph of MDD

vs fly ash content. Upto 20% of fly ash content MDD increased and then decreased. This is because the cation exchange between additives and expansive soil decreases the thickness of electric double layer and promotes the flocculation. The flocculation of the solid particles implies that the water-additives–soil mixtures can be compacted with lower water content, and the optimum water content is thus reduced. While decrease in the MDD of the mix with increase in fly ash content is basically because of the lower specific gravity of fly ash. Change in fly ash content vs variation of MDD and OMC are shown in fig-5.4a and fig-5.2 respectively.

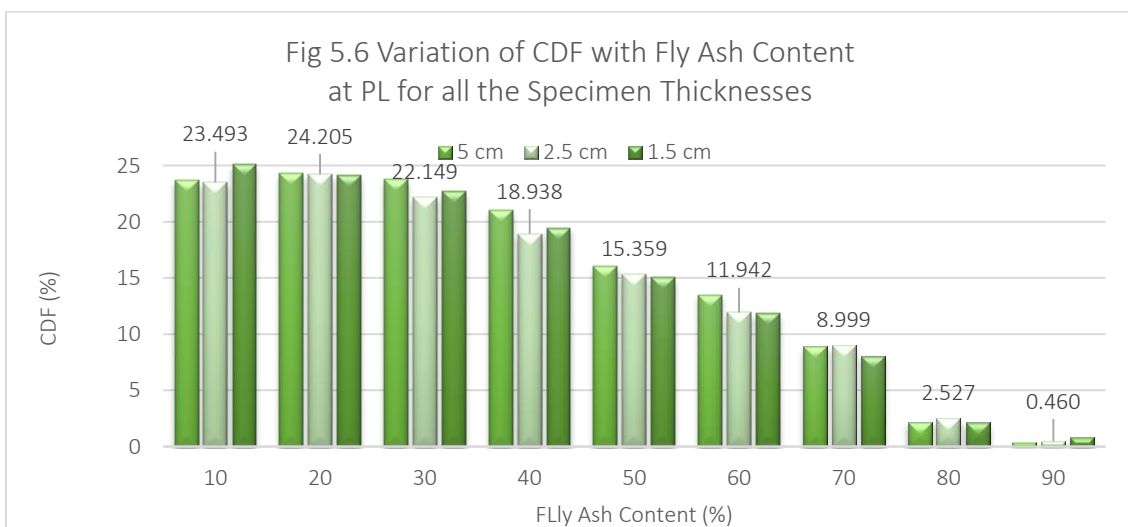
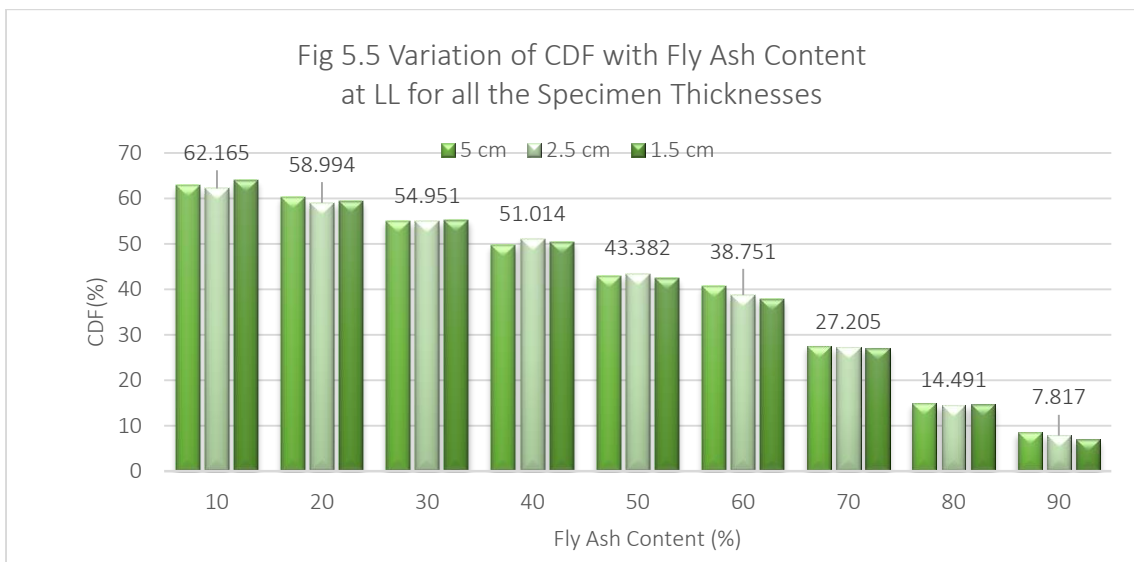


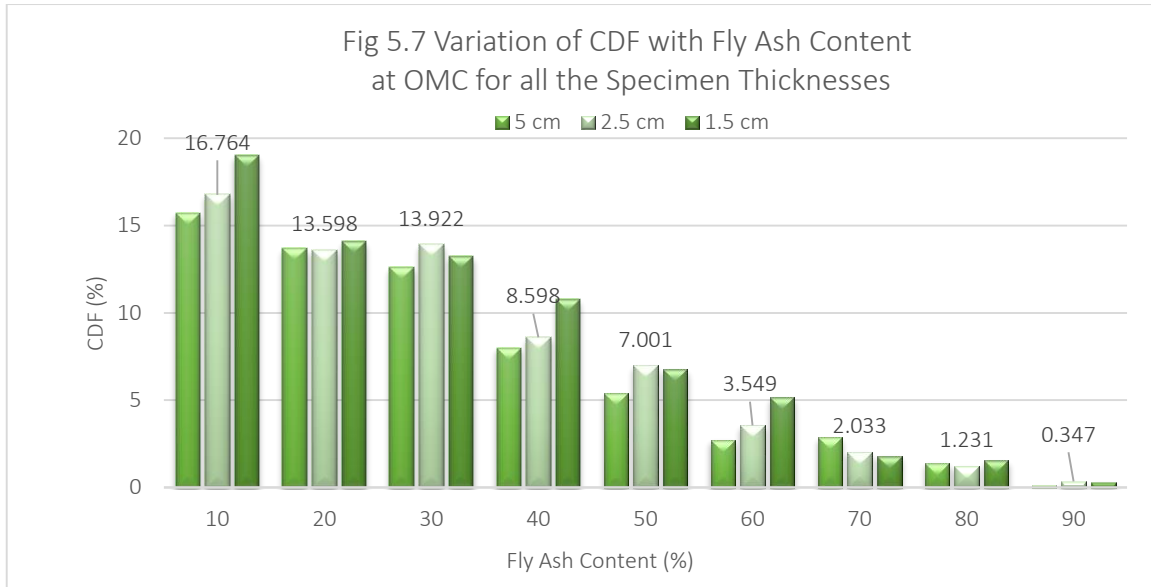
5.3 Determination of Cracking and Shrinkage Behaviour

5.3.1 Without Fibres

1. Variation of CDF with Fly Ash Content:

CDF is the percentage of surface shrinkage area (i.e. summation of cracks area and shrinkage area) in a specimen. From fig 5.5, 5.6 and 5.7 it can be clearly concluded that with the increase in fly ash content CDF is reducing consistently. Fly ash has very low shrinkage potential as discussed earlier. Addition of very low shrinking materials means reduction in the percentage of high shrinking materials in the mix. Therefore the percentage of overall surface shrinkage area (CDF) in the specimen is reduced as the fly ash content increases. This trend is followed for all the specimens whether they are at liquid limit, plastic limit or at OMC.





2. Variation of CDF with Moisture Content and Specimen Thickness:

Bentonites can retain a large amount of water. At constant fly ash content, higher moisture content in a specimen means low amount of solid soil particles. On the application of temperature, water will evaporate from the soil and the very small particles of bentonite clay will move radially inwards as they have high cohesion. This inward movement will be more if the percentage of water is more or the percentage of solid particles is less.

Increase in thickness leads to uneven drying of the layers of specimen, thus increases the surface cracks in a specimen. Fig 5.8 to fig 5.16 shows the variation of CDF with moisture contents and specimen thickness. For most of the specimens CDF increases with the increase in moisture content and thickness.

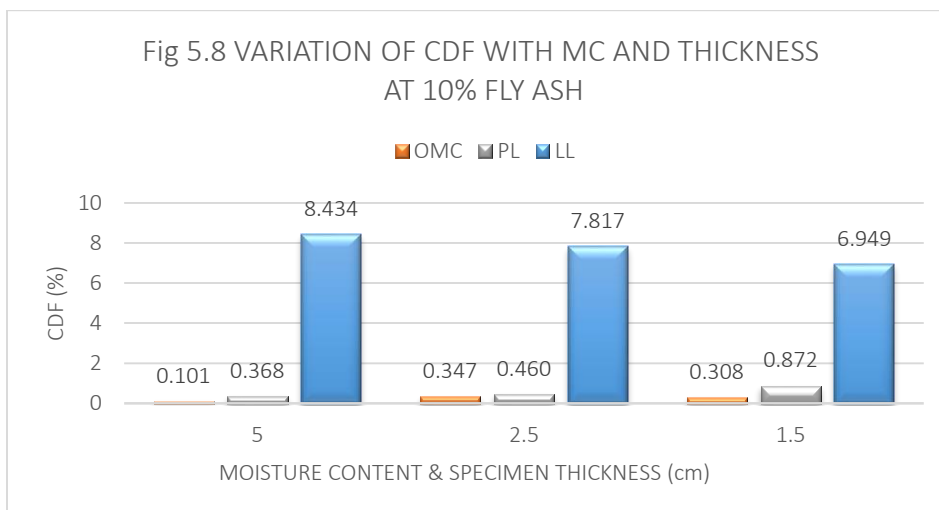


Fig 5.9 VARIATION OF CDF WITH M.C. AND THICKNESS AT 20% FLY ASH

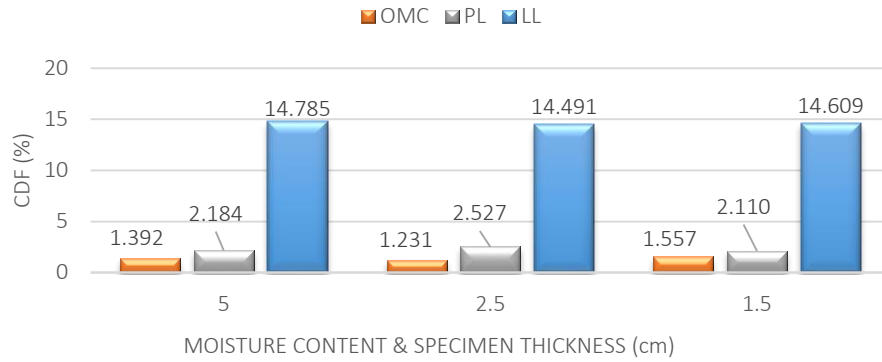


Fig 5.10 VARIATION OF CDF WITH MC AND THICKNESS AT 30% FLY ASH

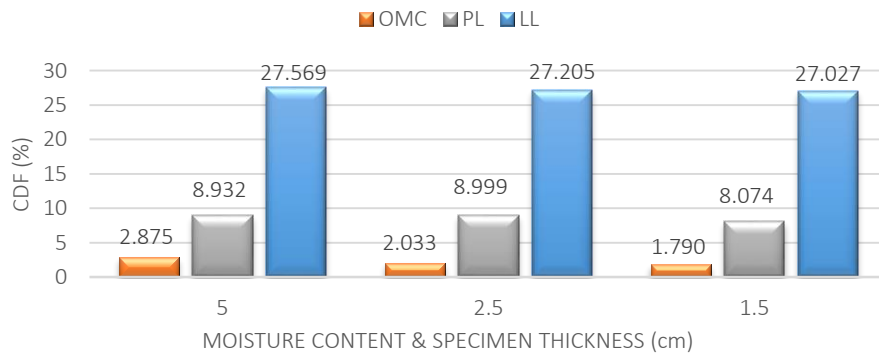


Fig 5.11 VARIATION OF CDF WITH MC AND THICKNESS AT 40% FLY ASH

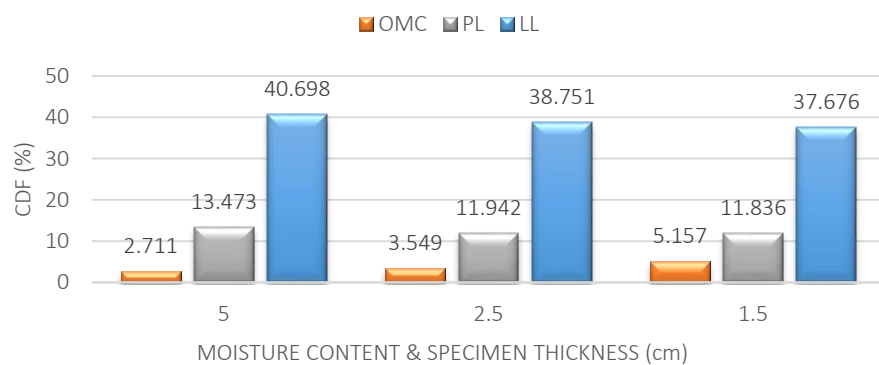


Fig 5.12 VARIATION OF CDF WITH MC AND THICKNESS AT 50% FLY ASH

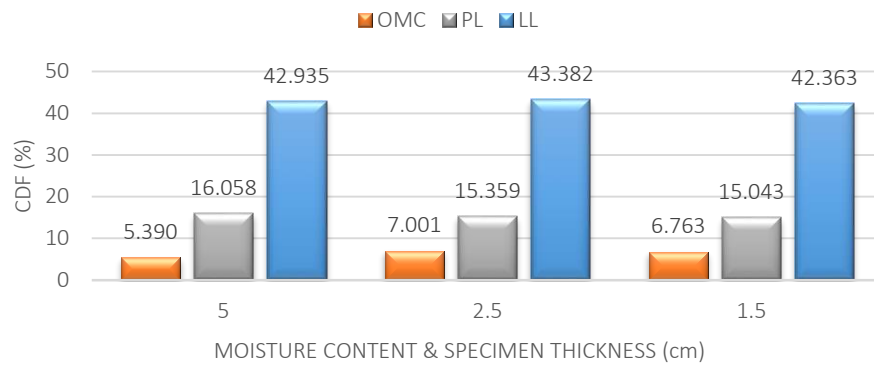


Fig 5.13 VARIATION OF CDF WITH MC AND THICKNESS AT 60% FLY ASH

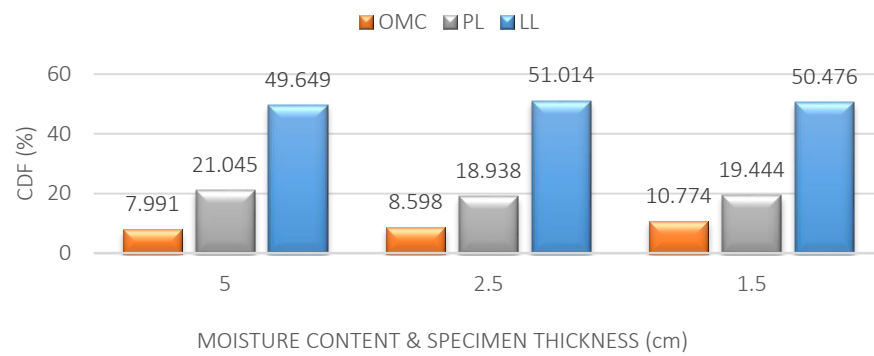
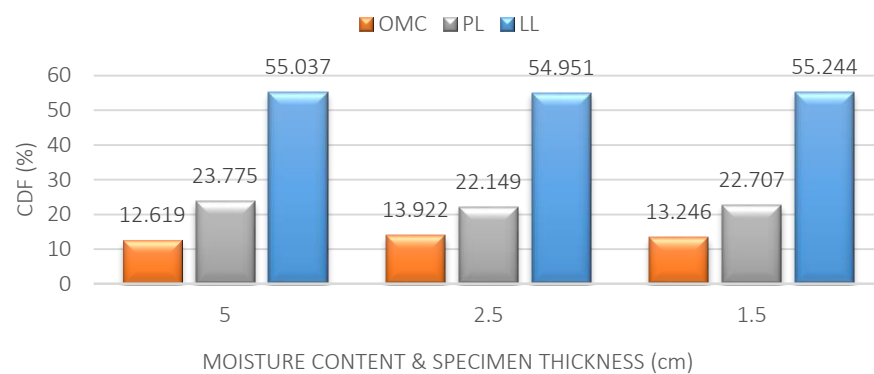
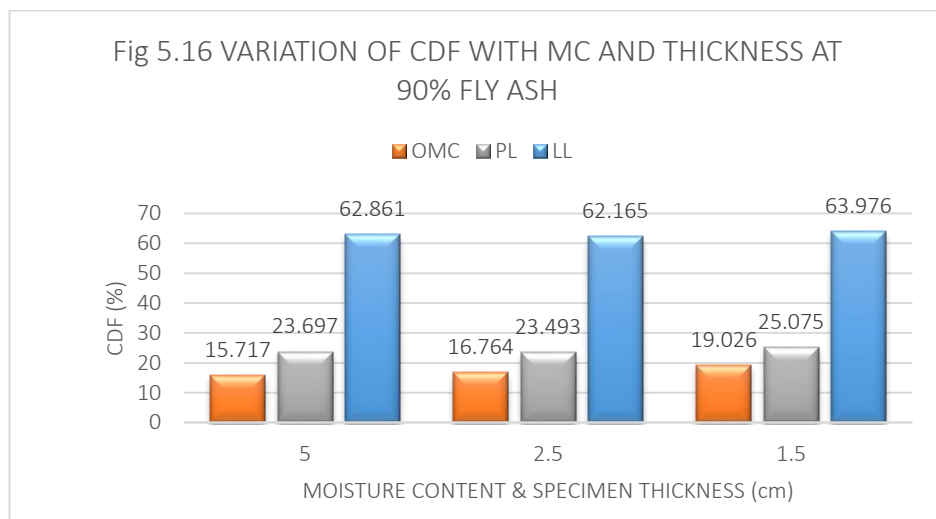
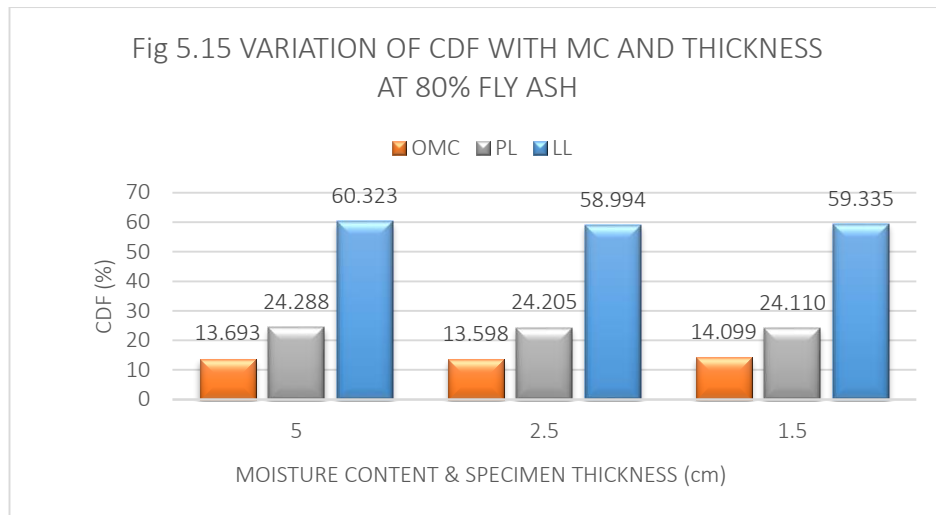


Fig 5.14 VARIATION OF CDF WITH MC AND THICKNESS AT 70% FLY ASH





3. Variation of CIF with Fly Ash Content:

CIF is the percentage of cracks in reduced specimen area. It generally decreases with the increase in fly ash content. Fly ash has very low capacity to swell and shrink. Thus the tensile stresses developed in the fly ash are very low. As a result it generally does not show cracks. With the increase in fly ash content in the mix shrinkage area is reduced and reduced specimen area is increased. Cracks were also reduced as a result we get low CIF. For fly ash content more than 70% cracks were disappeared. Hence for them CIF is zero. Variation of CIF with fly ash content is shown in figures 5.17, 5.18 and 5.19.

Fig 5.17 Variation of CIF with Fly Ash Content at LL for all the Specimen Thicknesses

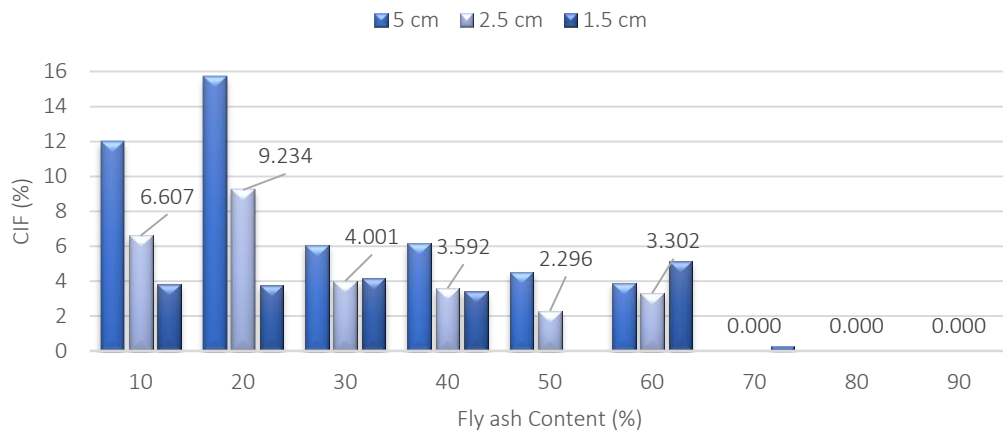
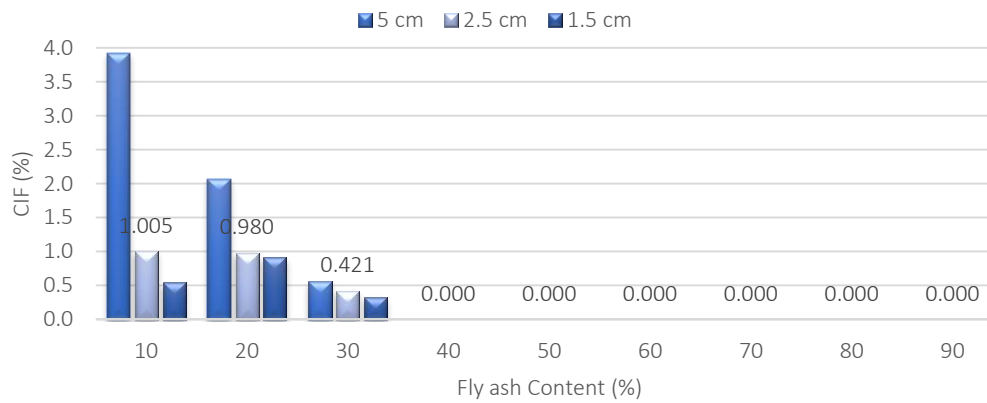
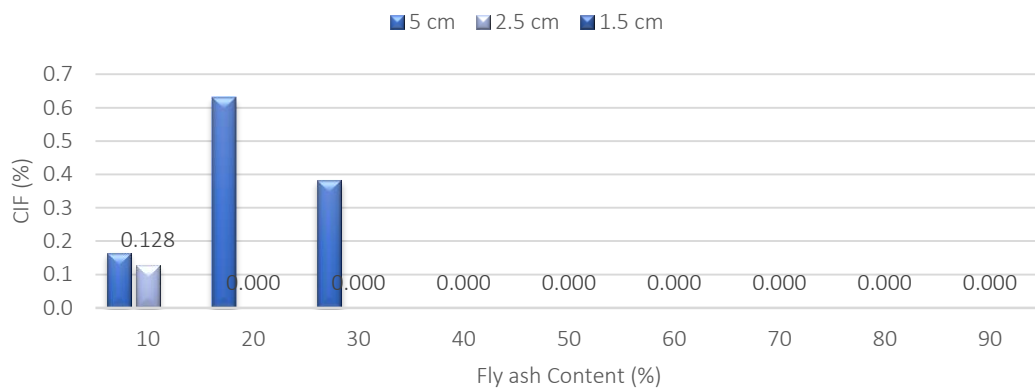


Fig 5.18 Variation of CIF with Fly Ash Content at PL for all the Specimen Thickness

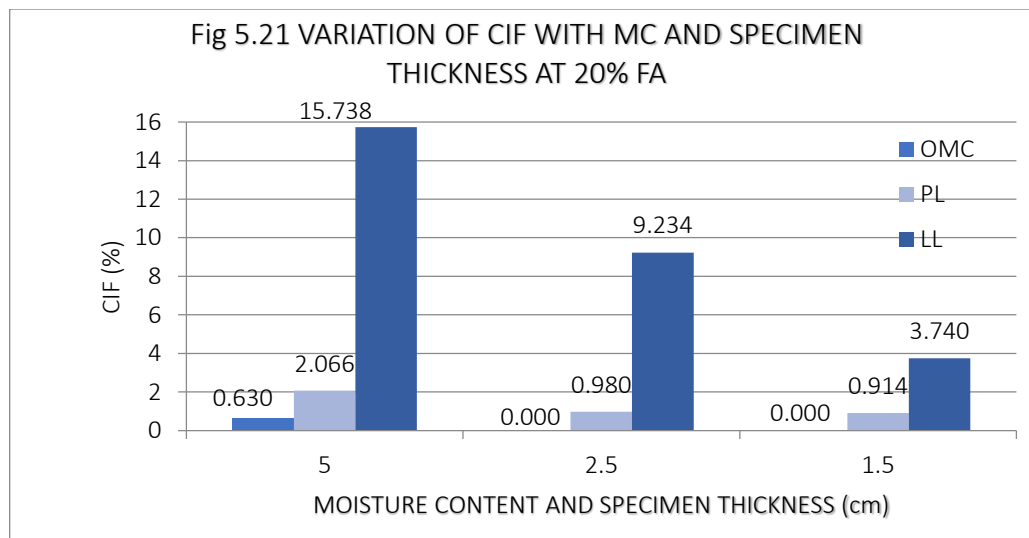
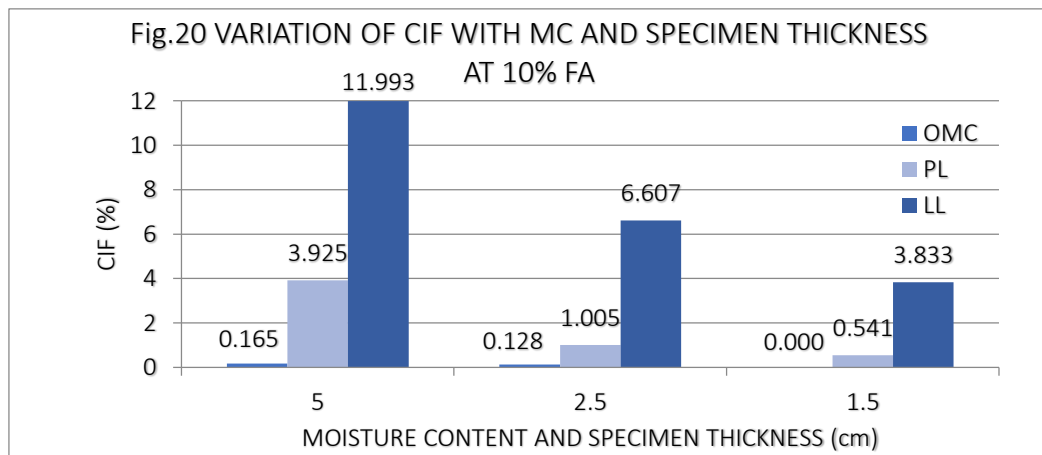


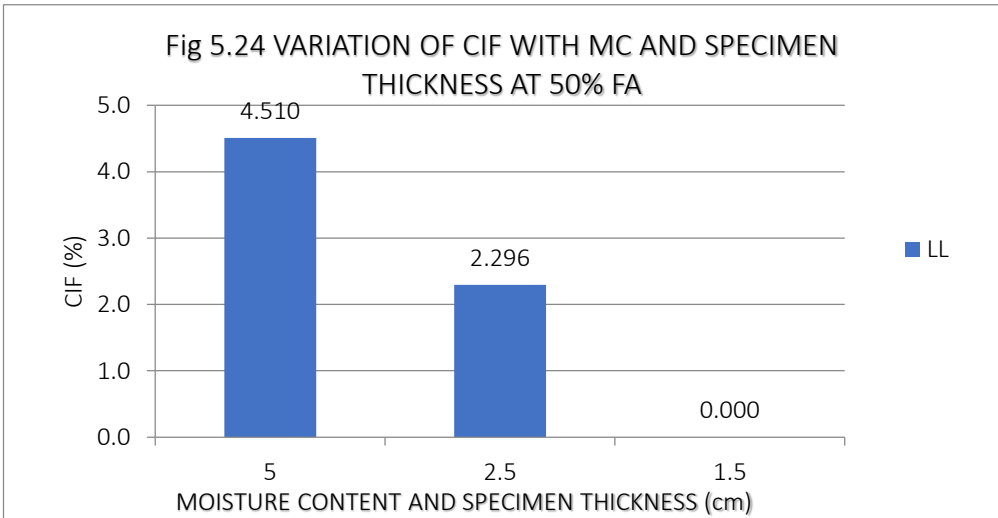
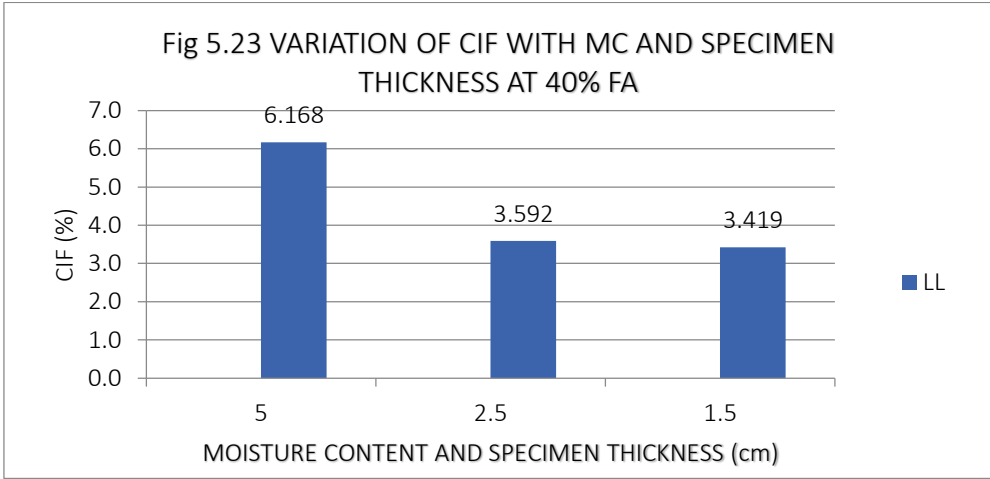
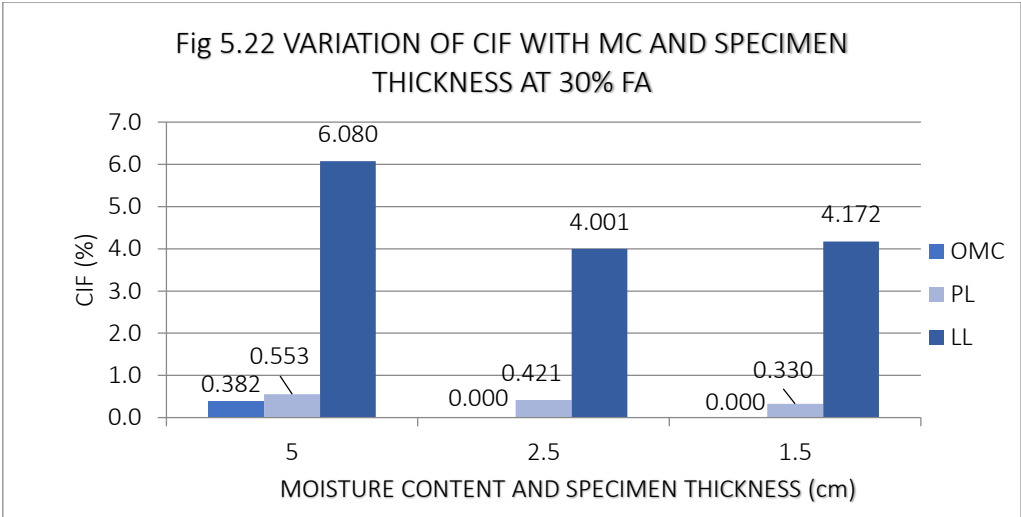
5.19 Variation of CIF with Fly Ash Content at OMC for all the Specimen Thickness

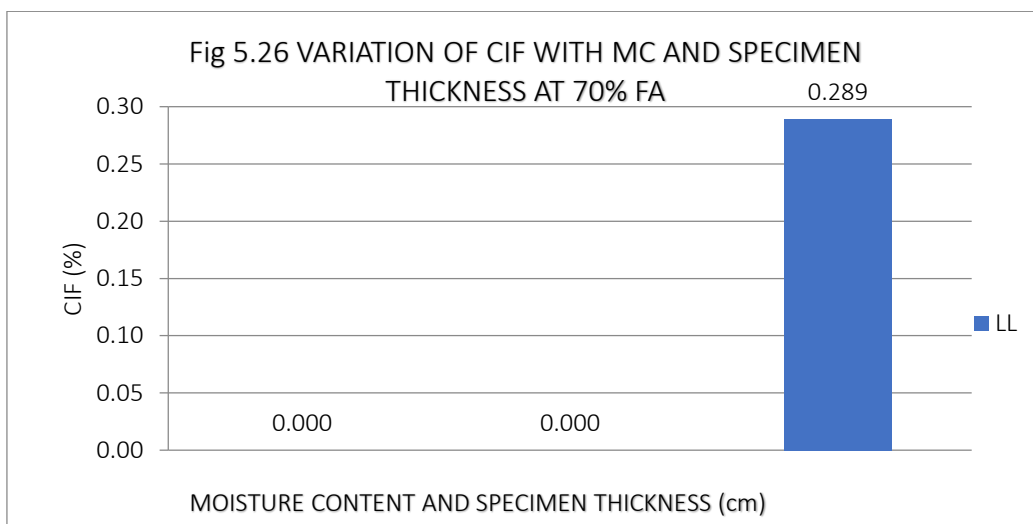
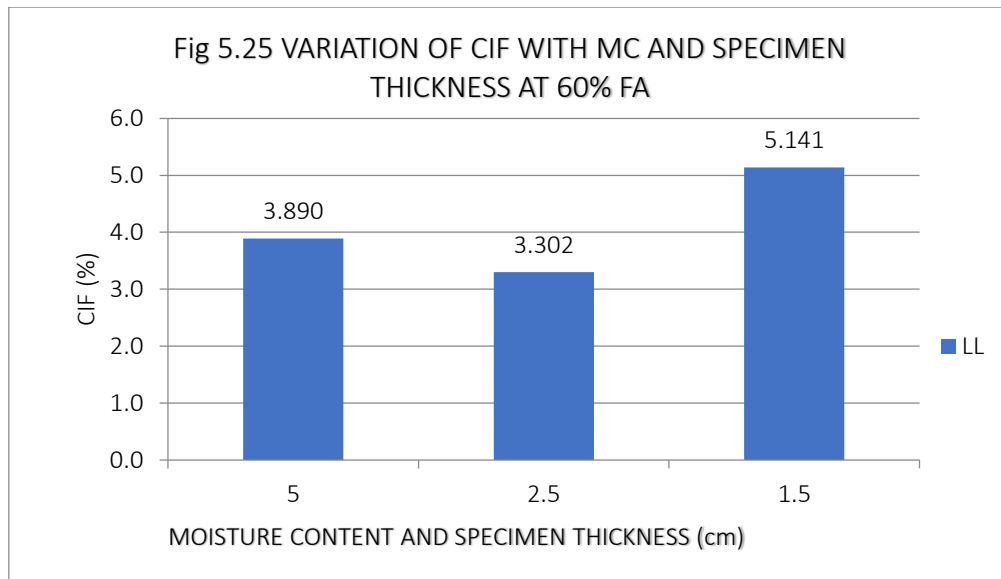


4. Variation of CIF with Moisture Content and Specimen Thickness:

Intensity of cracks increases with increase in water content and specimen thickness. For most of the specimens at OMC and plastic limit cracks were almost zero with more reduced specimen area. Hence for them CIF is 0. While for specimens at liquid limit or of more thickness cracks were more with low reduced specimen area. It accounts for the higher CIF value for those specimen. Variation of CIF with Moisture Content and Sample Thickness is shown in figures from 5.20 to 5.26.







For 80% and 90% fly ash CIF is zero for all the specimens

5. Variation of Cracks Area with Fly Ash Content:

Average cracks area reduces with increase in fly ash content for a fixed moisture content and specimen thickness as shown in fig 5.27, 5.28 and 5.29 because of the reasons mention earlier. Variation graph between cracks area with fly ash content at LL, PL and OMC are given below.

Fig 5.27 Variation of Cracks Area with Fly Ash Content at LL for all the specimen thickness

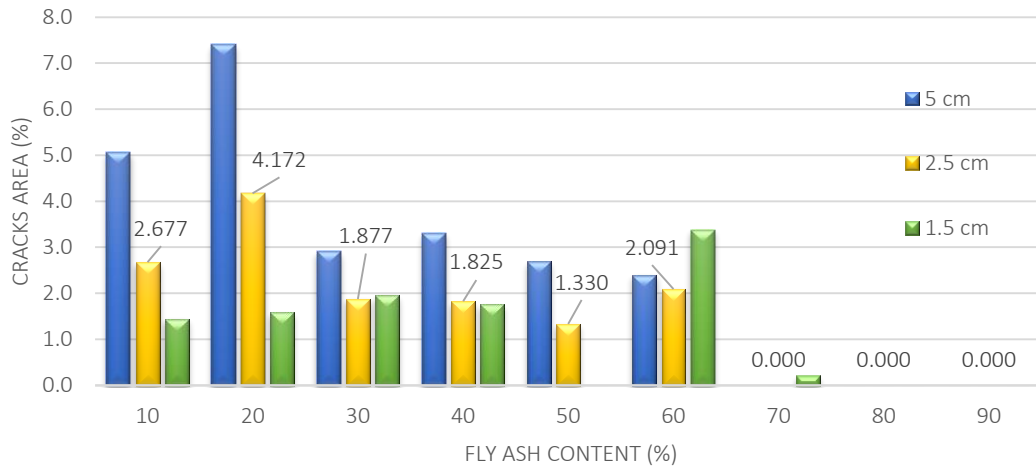


Fig 5.28 Variation of Cracks Area with Fly Ash Content at PL for all the specimen thickness

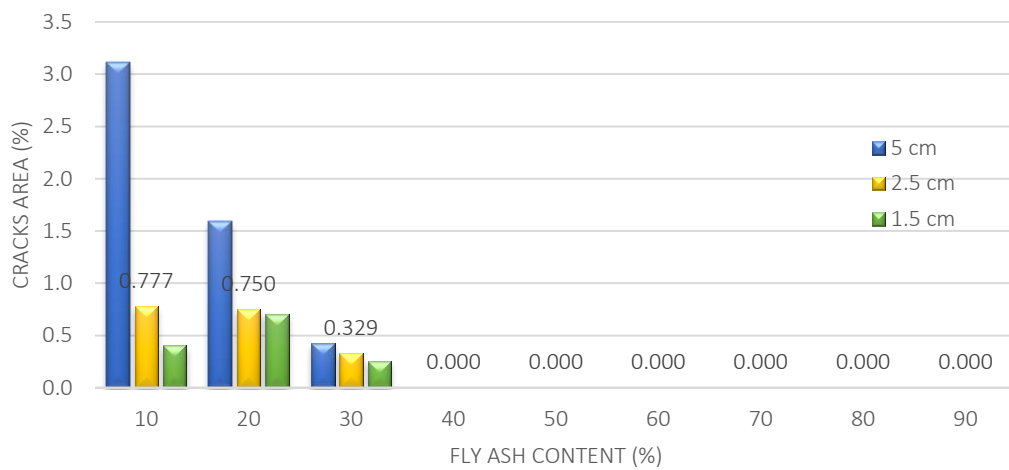
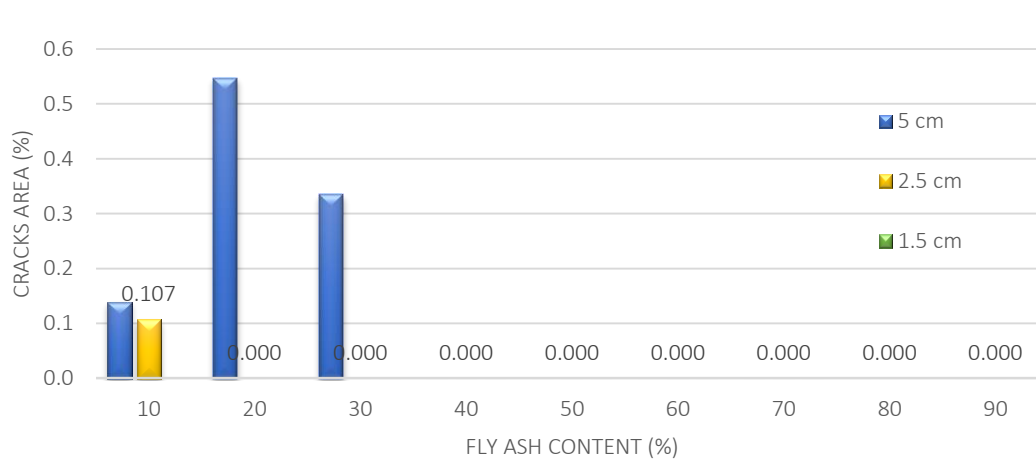
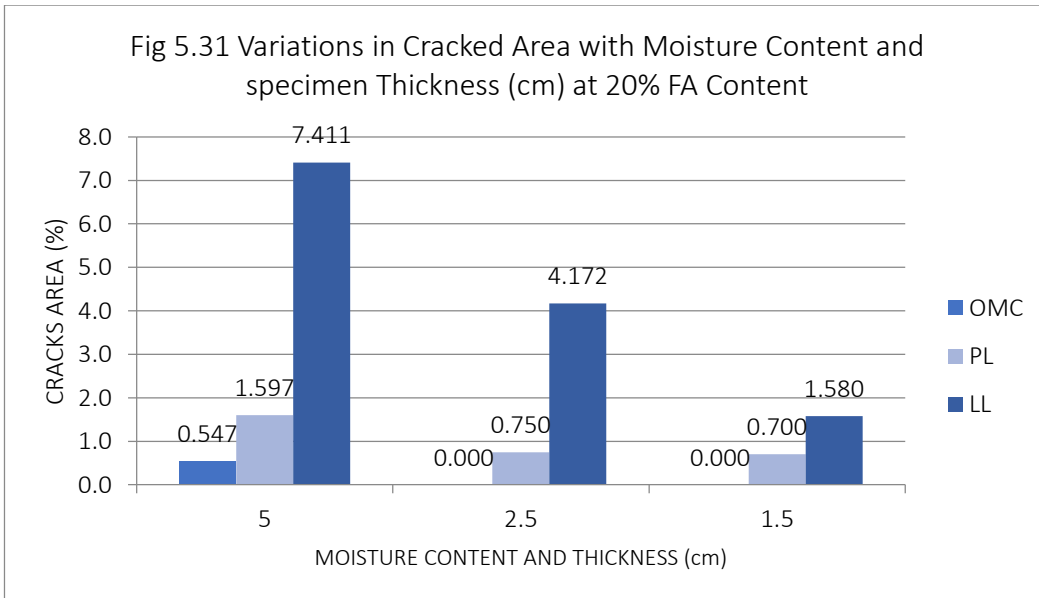
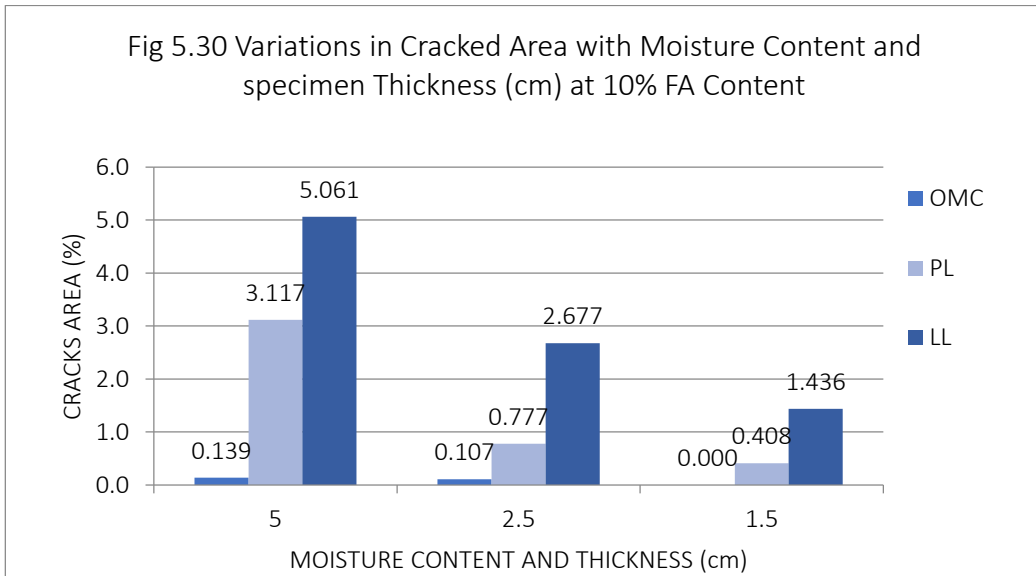


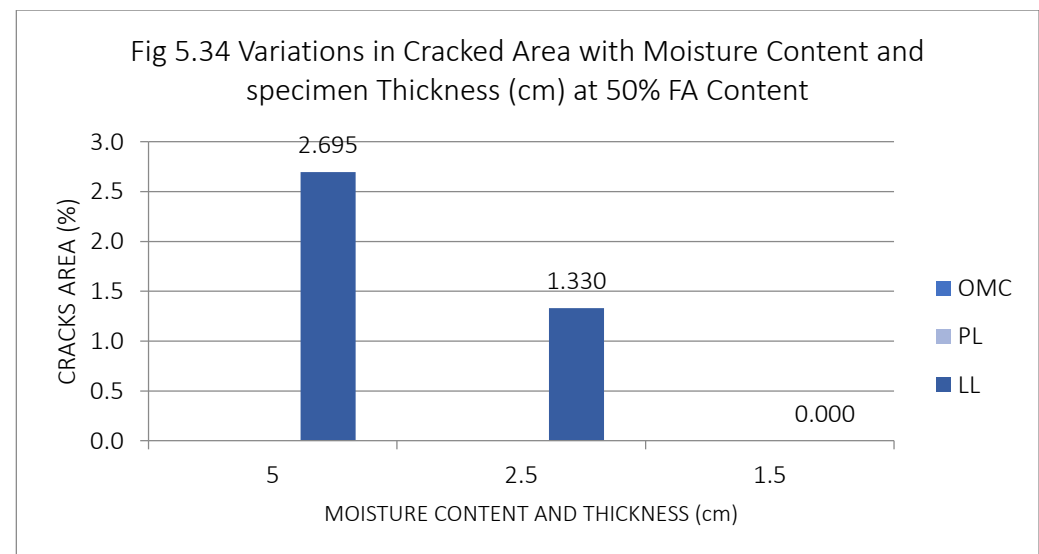
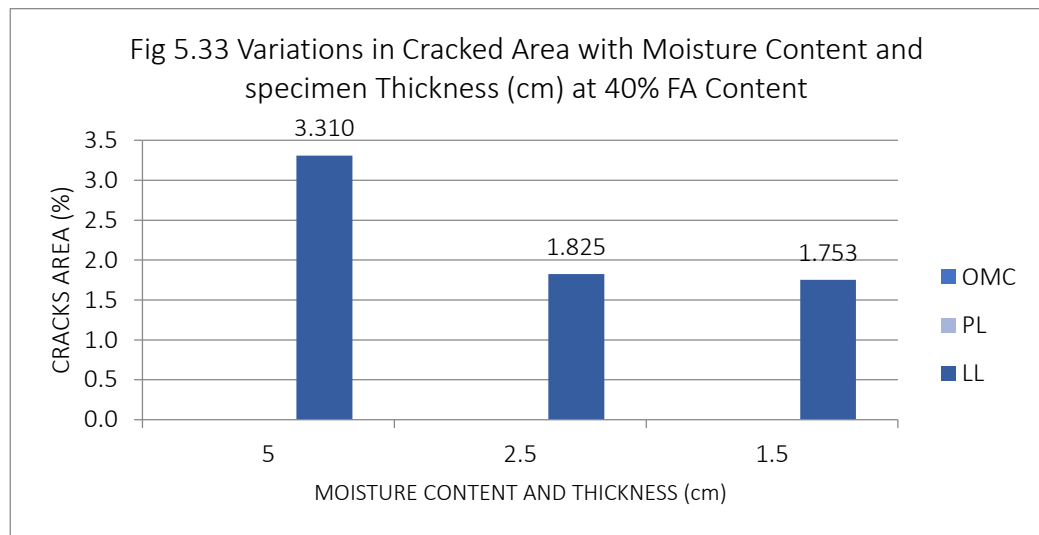
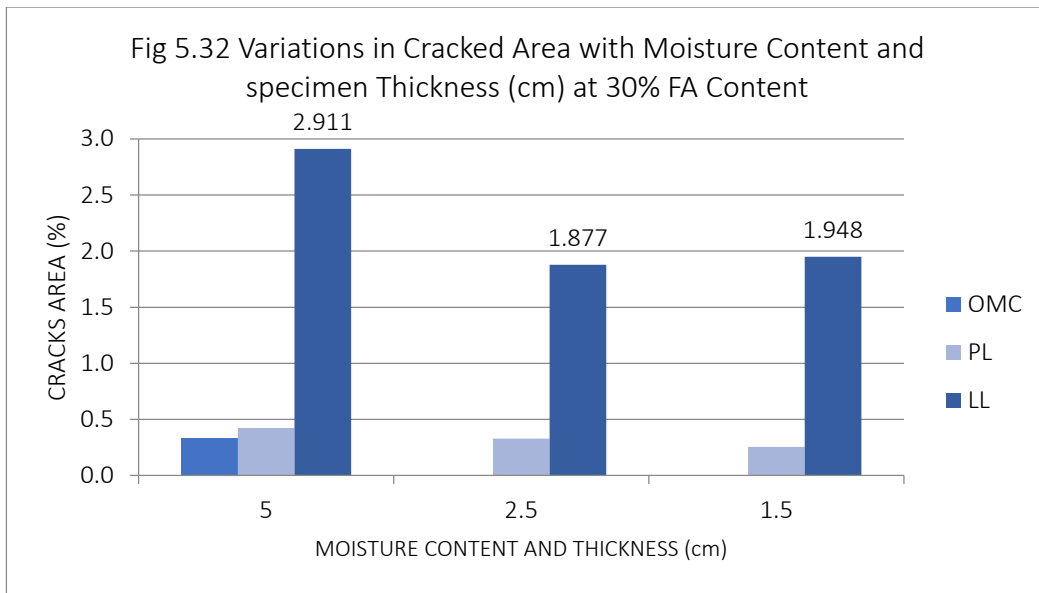
Fig 5.29 Variation of Cracks Area with Fly Ash Content at OMC for all the specimen thickness

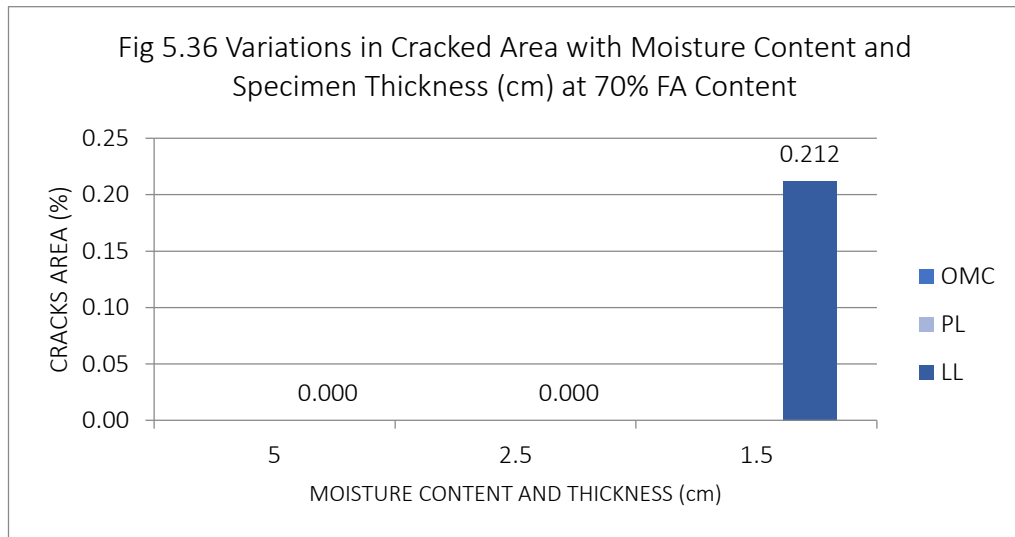
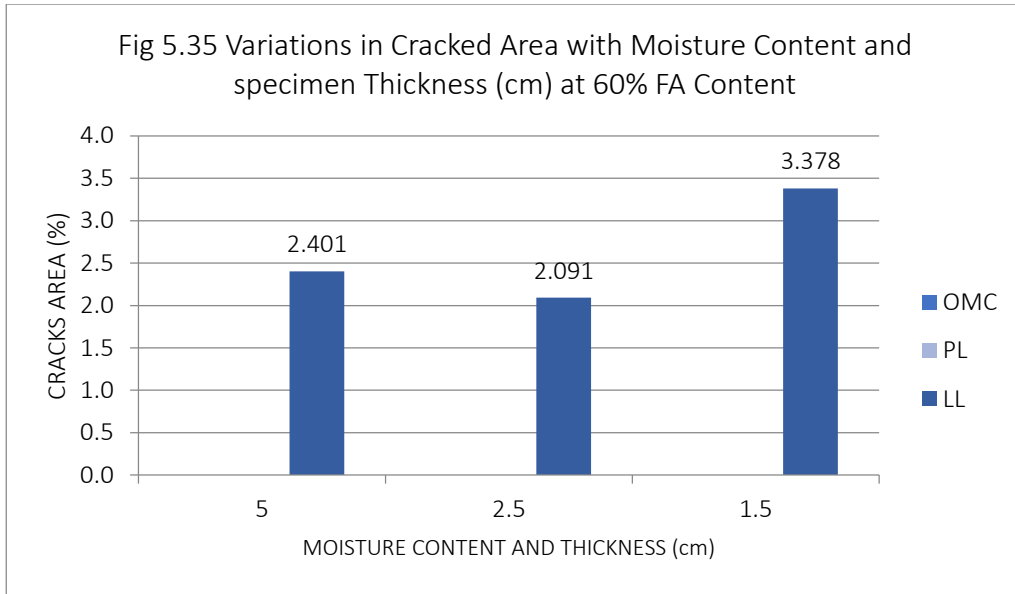


6. Variation of Cracks Area with Moisture Content and Specimen Thickness:

Cracked area is 0 for every specimen of mix having 80% and 90% fly ash. For specimens, cracked area increases with increase in moisture content and specimen thickness as mention in point no 2 above. Variation graphs of Cracks Area vs Moisture Content and Specimen Thicknesses are shown in fig 5.30 to 5.36.







7. Variation of Shrinkage Area with Fly Ash Content:

Shrinkage area decreases with the increase in fly ash content for most of the specimens. Variation graph of shrinkage area vs fly ash content is shown in figures 5.37, 5.38 and 5.39.

Fig 5.37 Variation of Shrinkage Area with Fly Ash Content at LL for all the specimen thickness

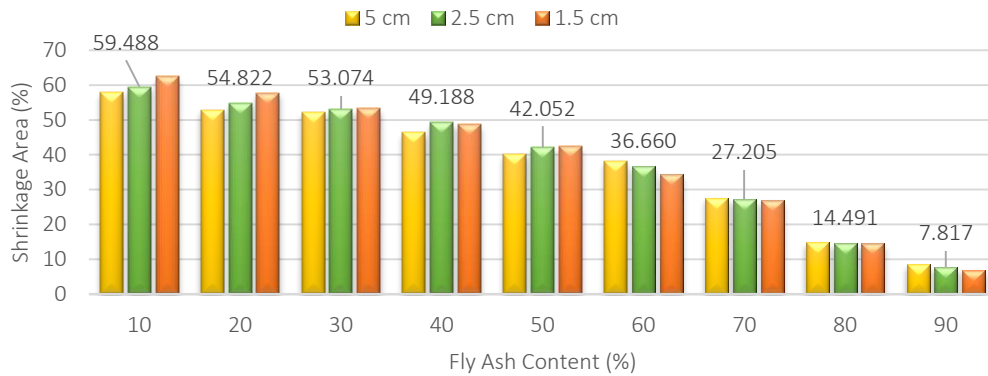


Fig 5.38 Variation of Shrinkage Area with Fly Ash Content at PL for all the specimen thickness

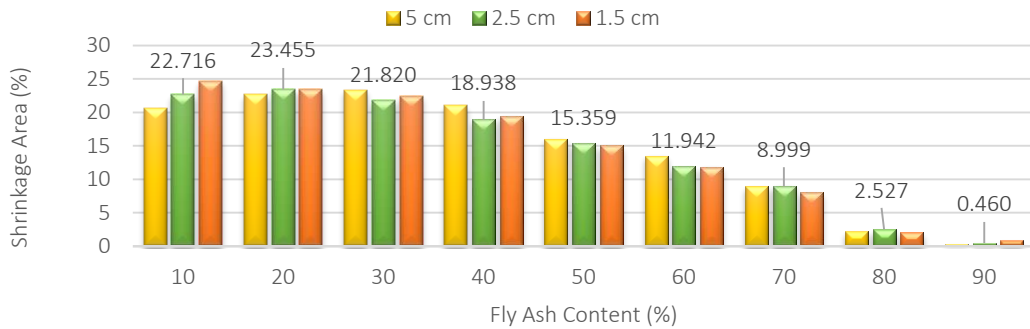


Fig 5.39 Variation of Shrinkage Area with Fly Ash Content at OMC for all the specimen thickness



8. Variation of Shrinkage Area with Moisture Content and Specimen Thickness

Shrinkage area increases with the increase in moisture content. But it does not show much variation with the specimen thickness. It is generally constant for all thicknesses.

Variation of Shrinkage Area with Specimen Thickness and Moisture Content at constant Fly Ash Content is shown in figures from 5.40 to 5.48

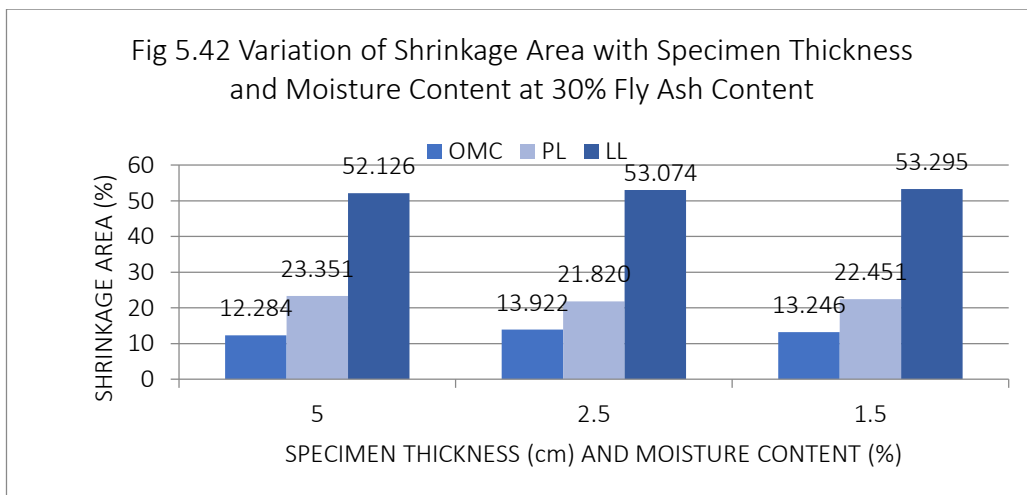
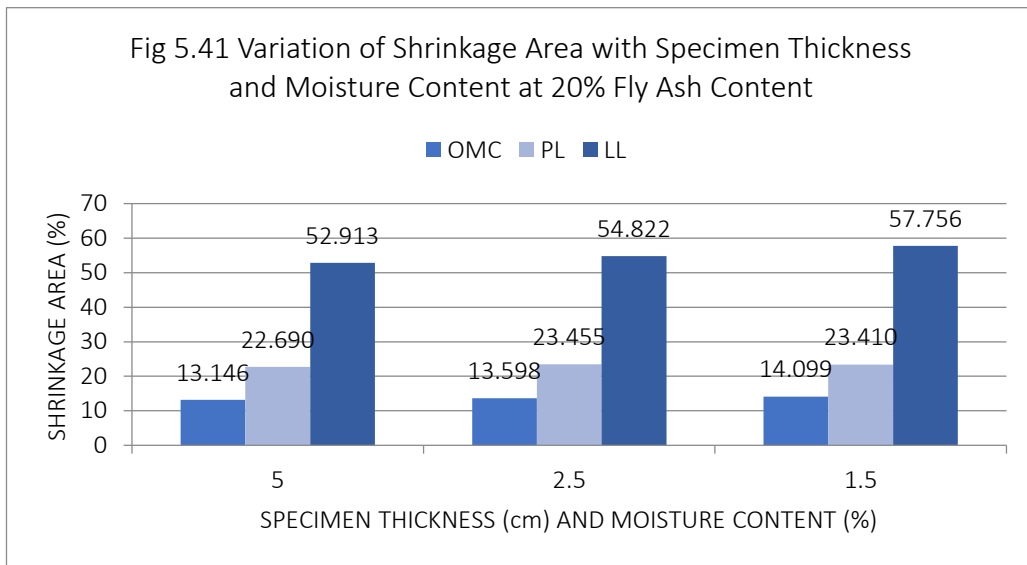
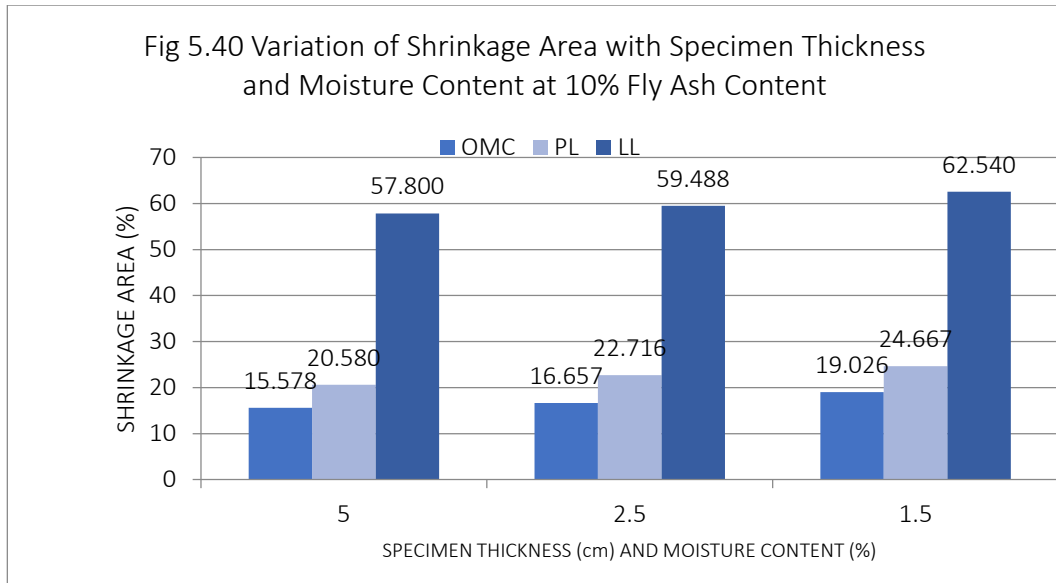


Fig 5.43 Variation of Shrinkage Area with Specimen Thickness and Moisture Content at 40% Fly Ash Content

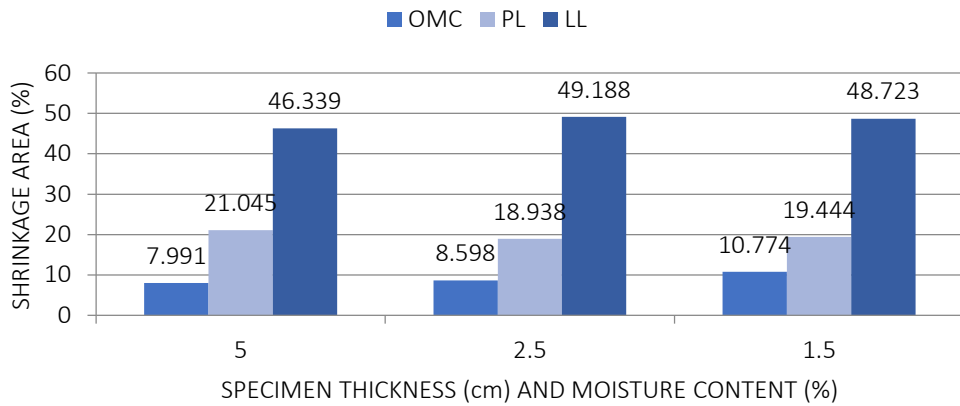


Fig 5.44 Variation of Shrinkage Area with Specimen Thickness and Moisture Content at 50% Fly Ash Content

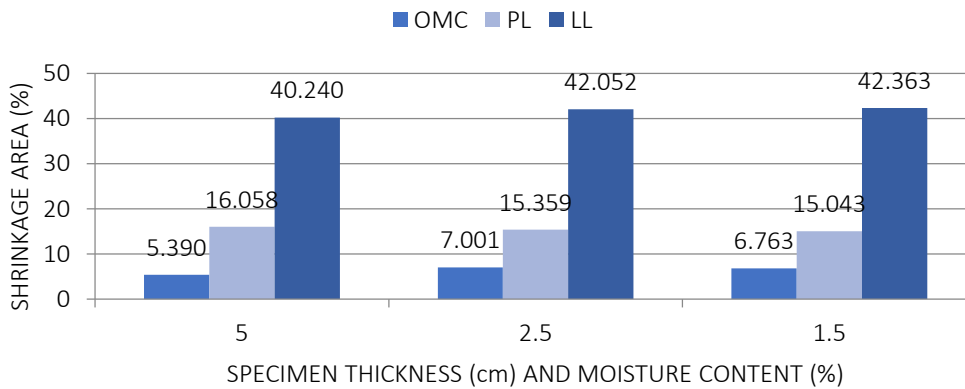


Fig 5.45 Variation of Shrinkage Area with Specimen Thickness and Moisture Content at 60% Fly Ash Content

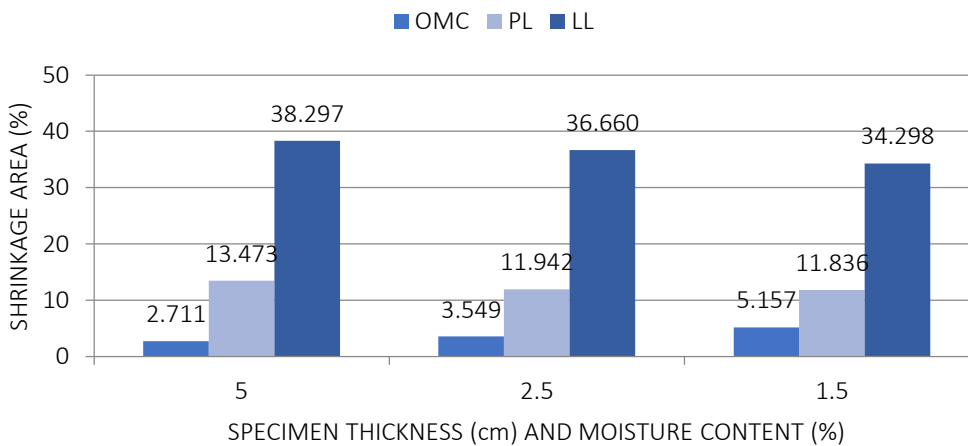


Fig 5.46 Variation of Shrinkage Area with Specimen Thickness and Moisture Content at 70% Fly Ash Content

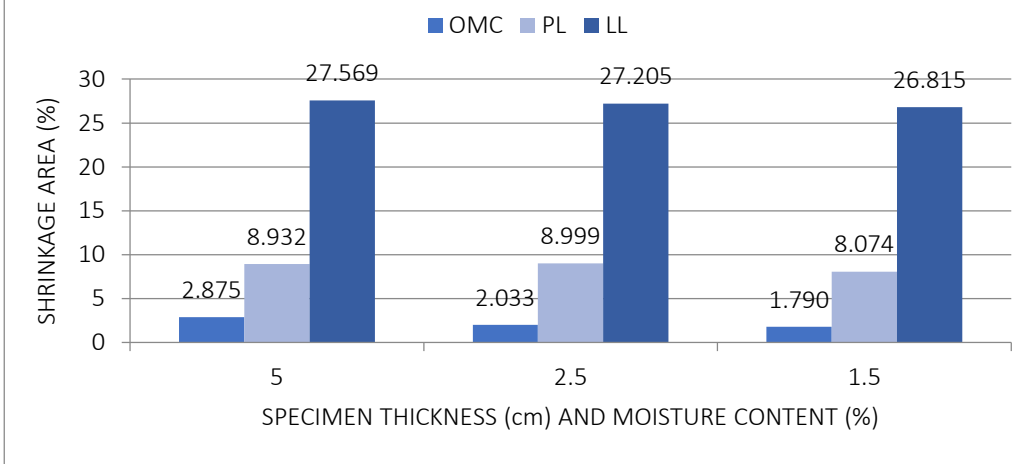


Fig 5.47 Variation of Shrinkage Area with Specimen Thickness and Moisture Content at 80% Fly Ash Content

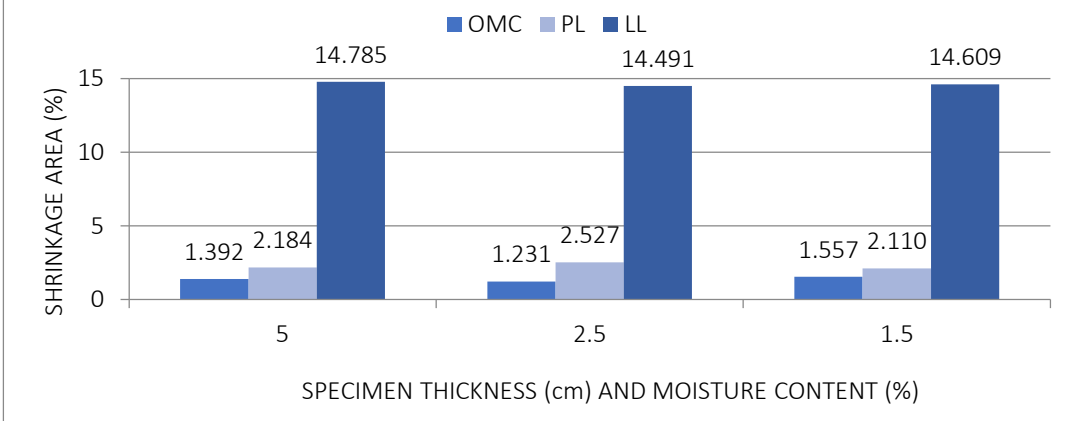
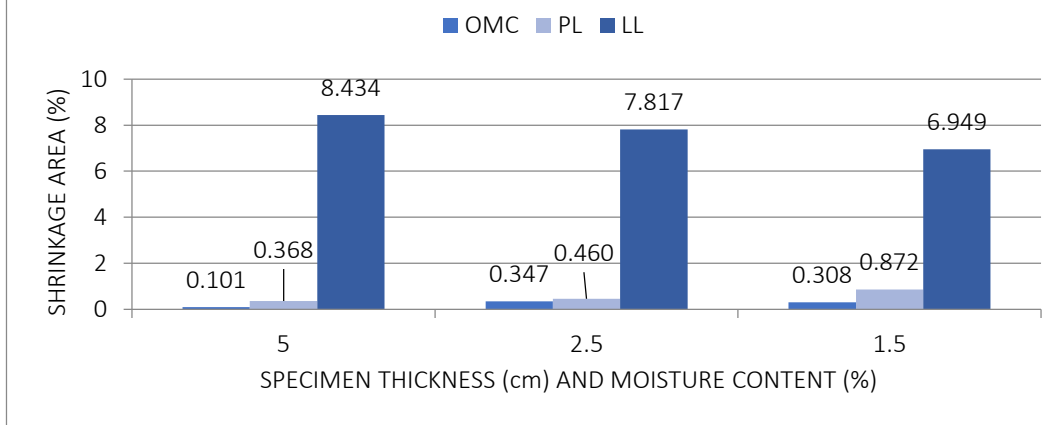


Fig 5.48 Variation of Shrinkage Area with Specimen Thickness and Moisture Content at 90% Fly Ash Content



5.3.2 Crack Length and Average Width of Cracks in Unreinforced Soil

Cracks total length and average width for each unreinforced specimen found is shown in table 5.1. The specimens which are not listed they did not show any cracks.

Table 5.1 Results of Total Cracks Length and Average Cracks Width of Unreinforced Soil

B/F MC SIZE Of Specimen	Total Cracks Length In (cm)	Average Cracks Width In (mm)
3070 LL S	10.446	0.269
4060 LL B	19.881	1.603
4060 LL M	34.378	0.807
4060 LL S	49.906	0.898
5050 LL B	26.297	1.360
5050 LL M	14.671	1.204
6040 LL B	41.272	1.064
6040 LL M	24.376	0.994
6040 LL S	13.759	1.691
7030 OMC B	33.378	0.133
7030 PL B	10.480	0.537
7030 PL M	14.698	0.297
7030 PL S	10.461	0.325
7030 LL B	38.691	0.999
7030 LL M	23.404	1.065
7030 LL S	17.313	1.494
8020 OMC B	33.378	0.133
8020 PL B	10.480	0.537
8020 PL M	14.698	0.297
8020 PL S	10.461	0.325
8020 LL B	38.691	0.999
8020 LL M	23.404	1.065
8020 LL S	17.313	1.494
9010 OMC B	10.803	0.171
9010 OMC M	18.361	0.077

9010 PL B	38.343	1.079
9010 PL M	0.230	0.230
9010 PL S	0.317	0.317
9010 LL B	1.525	1.525
9010 LL M	0.572	0.674
9010 LL S	0.298	0.895

5.3.3 With 2% recron©3s, 6mm Fibres

1. Variation of CDF with addition of fibres content in the above mixes.

A direct comparison of CDF value in the mix tested before the application of reinforcement and after the application of reinforcement is given in the table 5.2 below. F/B stands for fly ash/ bentonite ratios, MC for moisture content, LL for liquid limit, PL for plastic limit, B SIZE for 5cm, M SIZE for 2.5cm and S SIZE for 1.5cm.

Table 5.2 Comparison of CDF for Reinforced and Unreinforced Soil

F/B MC SIZE Of Specimen	CDF (%) WITHOUT FIBRES	CDF (%) WITH FIBRES	F/B MC SIZE Of Specimen	CDF (%) WITHOUT FIBRES	CDF (%) WITH FIBRES
9010 LL B	62.861	44.759	8020 LL B	60.323	40.099
9010 LL M	62.165	45.794	8020 LL M	58.994	43.884
9010 LL S	63.976	48.016	8020 LL S	59.335	41.580
9010 PL B	23.697	19.352	8020 PL B	24.288	16.751
9010 PL M	23.493	18.439	8020 PL M	24.205	17.746
9010 PL S	25.075	16.898	8020 PL S	24.110	17.013
7030 LL B	55.037	35.303	6040 LL B	49.649	41.759
7030 LL M	54.951	35.201	6040 LL M	51.014	38.058
7030 LL S	55.244	36.439	6040 LL S	50.476	34.256
7030 PL B	23.775	17.071	6040 PL B	21.045	17.571
7030 PL M	22.149	17.199	6040 PL M	18.938	14.427
7030 PL S	22.707	15.655	6040 PL S	19.444	12.002

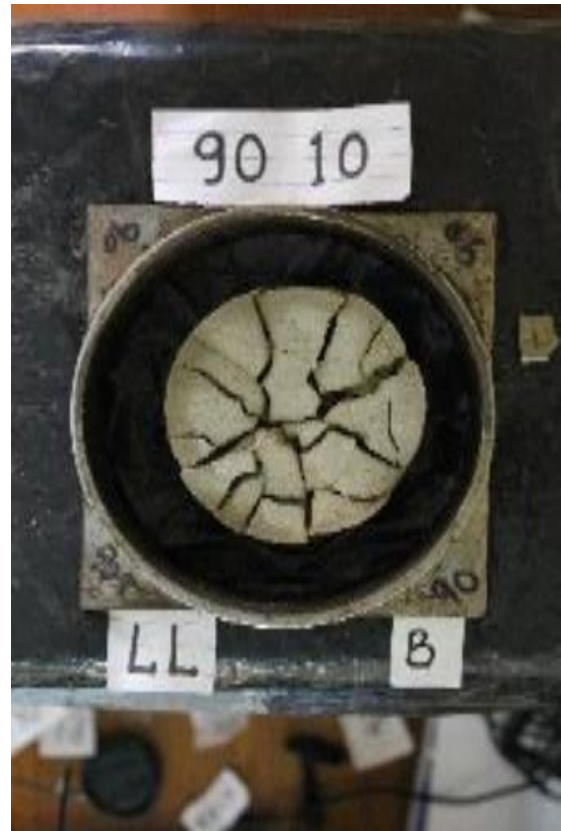
5050 LL B	42.935	34.369	4060 LL B	40.698	30.290
5050 LL M	43.382	32.400	4060 LL M	38.751	26.782
5050 LL S	42.363	28.926	4060 LL S	37.676	23.697
5050 PL B	16.058	12.676	4060 PL B	13.473	9.844
5050 PL M	15.359	10.768	4060 PL M	11.942	9.970
5050 PL S	15.043	10.253	4060 PL S	11.836	8.324
3070 LL B	27.569	15.024	2080 LL B	14.785	10.552
3070 LL M	27.205	14.584	2080 LL M	14.491	8.320
3070 LL S	27.027	13.961	2080 LL S	14.609	10.494
3070 PL B	8.932	6.516	2080 PL B	2.184	3.913
3070 PL M	8.999	7.694	2080 PL M	2.527	4.532
3070 PL S	8.074	5.804	2080 PL S	2.110	3.942
1090 LL B	8.434	7.351	1090 PL B	0.368	3.260
1090 LL M	7.817	6.714	1090 PL M	0.460	3.846
1090 LL S	6.949	5.895	1090 PL S	0.872	2.021

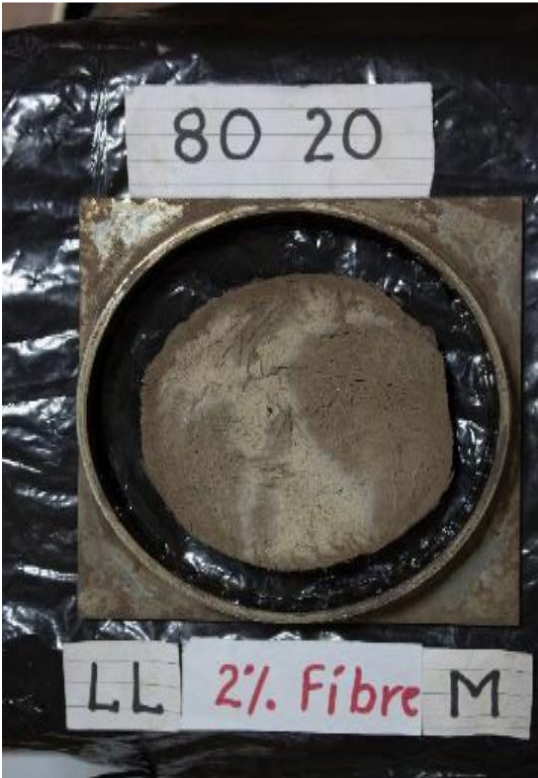
From table above we can observe that for reinforced specimens prepared at liquid limit CDF (%) value has decreased consistently. For the mix of higher bentonite content, fibres work very well as proper bonding is there in between the surface area of fibres and bentonite particles which resist the inward movement of particles and reduces surface shrinkage area (CDF) upto upto 30% while for mix of higher fly ash content bonding is not that much ,therefore CDF is reduced by only 13%.

Specimen prepared at plastic limit with higher bentonite content showed reduction of 17% in CDF value. But for specimens at 80% and 90% fly ash content showed negative affect with the introduction of fly ash. CDF value increased many times. This is because fly ash is non cohesive material and hence interlocking of particles is absent in the mix. They do not make proper bonding with fibres, infact they decrease the compacting density of soil. Therefore addition of fly ash does not contribute to the shrinkage reduction but increment in CDF for higher percentages of fly ash content.

Comparison Picture of Reinforced and Unreinforced Bentonite- Fly Ash Mixes







CHAPTER 6

CONCLUSIONS

6.1 Summary

The main objectives of the present research were identified as follows:

1. To study the geotechnical properties of different bentonite-fly ash mixes and to find out the changes that take place in them with increase in fly ash content.
2. To develop a new methodology that can be used for the quantification of cracks and shrinkage.
3. To study the trend followed by cracks and shrinkage with increase in fly ash content, moisture content and specimen thickness in the different mixes.

To achieve the above objectives, various tests like shrinkage limit test, liquid limit test, plastic limit test, specific gravity test and standard proctor compaction tests were performed. An extensive experimental program has been undertaken in the laboratory to develop a new methodology for the quantification of cracks and shrinkage. Soils were artificially prepared by mixing fly ash in bentonite in various proportions. Effect of moisture content and specimen thickness in cracking and shrinkage characteristics were observed.

6.2 Conclusions

Based on the experimental investigations following conclusions can be made

1. Specific Gravity was more for bentonite as compared to fly ash. Therefore as the percentage of fly ash in the bentonite-fly ash mix increased, its specific gravity was reduced.
2. Liquid limit, plastic limit and plasticity index decreased with the increase in fly ash content in the mix.
3. Shrinkage limit increases with the increase in fly ash content in the mix.
4. Addition of fly ash upto 20%, increases the maximum dry density of mix initially. Above that percentage MDD is reduced considerably. While OMC is initially decreased upto 20% fly ash content and then increased.
5. Shrinkage area and cracks area were reduced with the increase in fly ash content in the bentonite-fly ash mix.

6. With the increase in moisture content or specimen thickness, shrinkage and cracks area were increased.
7. CDF and CIF for the specimens were decreased with the increase in fly ash content and increased with the increase in moisture content or specimen thickness.

6.3 Future Work

1. In present work, study on the effect of variable parameters like fly ash content, moisture content and specimen thickness on soil cracking and shrinkage was done. It can further be extended by considering some other variable parameters like the effect of fibres content, fibre size, rate of curing, suction cycles on cracks and shrinkage.
2. This work can be extended to study the cracking behaviour in other different types of soil as this method does not depend on the materials.
3. Cracking is basically a 3-D phenomena, so the depth determination of cracks is equally important. No methods are available in literatures to find the average depth of cracks. A new method can be develop to find the depth of cracks.
4. Image analysis technique can be extended to study the micro structural change in the soil on the application of chemicals, stabilizers or admixtures. Thus strength of soil can be predicted based on the type of micro structures they formed.
5. Swelling behaviour can also be study by image analysis technique.
6. This method can even be applied to other engineering fields like bio technology, minning, agriculture, geology etc for research work.

References

- Anand J. Puppala, Balakrishna Katha, and Laureano R. Hoyos., (2004): Volumetric Shrinkage Strain Measurements in Expansive Soils Using Digital Imaging Technology, *Geotechnical Testing Journal*, Vol. 27, No. 6, Paper ID GTJ12069.
- Auvray, R., Rosin-Paumier, S., Abdallah, A., and Masrouri, F. (2014). Quantification of soft soil cracking during suction cycles by image processing. *European Journal of Environmental and Civil Engineering*, Vol. 18, No. 1, 11–32.
- Azadegan, Omid. (2012). Laboratory Study on the Swelling, Cracking and Mechanical Characteristics of the Palm Fiber Reinforced Clay. *EJGE*, vol. 17, pp. 47-54.
- Bose, Bidula. (2012). Geo-Engineering Properties of Expansive Soil Stabilized with Fly Ash. *EJGE*, vol. 17, pp. 1339-1353.
- Lakshmikantha, M., Prat, P., & Ledesma, A. (2009). Image analysis for the quantification of a developing crack network on a drying soil. *Geotechnical Testing Journal*, 32, 505–515.
- Laskar, Arpan., Pal, Kumar, Sujit. (2013). Effect of random inclusion of waste plastic fibers on engineering behaviours of reinforced soil. *Indian Geotechnical Conference December 22-24, 2013, Roorkee*.
- Lim, B. F. and Siemens, G. A., “An Unconfined Swelling Test for Clayey Soils That Incorporates Digital Image Correlation,” *Geotechnical Testing Journal*, Vol. 36, No. 6, 2013, pp. 1–11, doi:10.1520/GTJ20120220. ISSN 0149-6115.
- Mahmoud R. Maheri , Alireza Maheri , Saeed Pourfallah , Ramin Azarm & Akbar Hadjipour (2011) Improving the Durability of Straw-Reinforced Clay Plaster Cladding for Earthen Buildings, *International Journal of Architectural Heritage: Conservation, Analysis, and Restoration*, 5:3, 349-366, DOI:10.1080/15583051003663859
- Mir, B. A. (2013). Effect of fly ash on swelling potential of BC soil. *Indian Geotechnical Conference December 22-24, 2013, Roorkee*.
- Phanikumar, B. R., and Radhey S. Sharma, M. ASCE (2007): Volume Change Behavior of Fly Ash-Stabilized Clays, *Journal of Materials in Civil Engineering*, Vol. 19, No. 1, pp. 67-74, DOI: 10.1061/_ASCE_0899-1561_2007_19:1_67_
- Srivastava, Amit, Pandey, Shikha., & Rana, Jeeshant. (2014). Use of shredded tyre waste in improving the geotechnical properties of expansive black cotton soil. *Geomechanics and Geoengineering: An International Journal*, DOI: 10.1080/17486025.2014.902121.
- Stephen G. Fityus, Donald A. Cameron, and Paul F. Walsh, (2005): The Shrink Swell Test, *Geotechnical Testing Journal*, Vol. 28, No. 1, Paper ID GTJ12327
- Subba Rao, K. S. and Satyadas, G. C., “Measurement of Volumetric and Linear Shrinkage on Black Cotton Soil,” *Geotechnical Testing General*, GTJODJ, vol. 8, no. 2, June 1985, pp. 66-70.

Uzan, Jacob, "An Apparatus for Two-Dimensional Measurement of the Shrinkage Resistance of Soils," *Journal of Testing Evaluation*, JTEVA, Vol. 2, No. 6, Nov. 1974, pp. 489-495.

Yudhbir, and Abedinzadeh, R., "Quantification of Particle Shape and Angularity Using the Image Analyser," *Geotechnical Testing General*, GTJODJ, Vol. 14, No. 3, September 1991, pp. 296-308.